Electroweak measurements with high statistics LHC data

Takanori Kono (Ochanomizu University)

on behalf of ATLAS and CMS collaborations

Physics in Collisions 2023

Tarapaca University, 2023.10.10 – 13

Electroweak symmetry breaking

- Electroweak symmetry breaking (EWSB) has several phenomenological implications
  - Higgs particle and gauge boson masses (m_W, m_Z)
  - Interactions of gauge bosons ($\bar{\Psi}V_\mu\Psi, VVV, VVVV, VVH$)
  - Fermion masses and Yukawa couplings to Higgs particle

- Measurements of these properties to confirm the validity of the Standard Model (SM) are important to understand the physics at the TeV scale
  - Deviations in any of these properties would require an extension to the SM, in particular the origin of EWSB

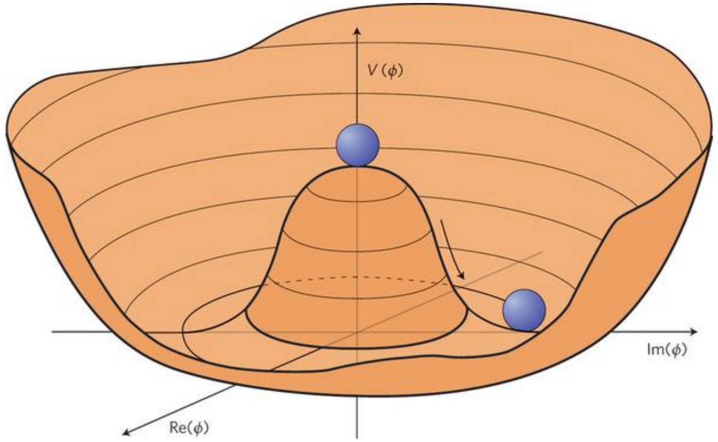

$$V(\Phi) = -\mu^2|\Phi| + \lambda|\Phi|^2$$

Vector boson scattering

- The EW vector boson scattering (VBS) is an essential tool to probe the origin of EWSB
  - Longitudinally polarized vector boson scattering amplitudes are kept finite by the contribution of the Higgs boson
  - Longitudinal components of $W^{\pm}, Z^0$ bosons originate from the components of the Higgs doublet field
- Measurement of the longitudinally polarized VBS is an important program at the LHC
- Effects of physics beyond the SM (BSM) can be incorporated in Effective Field Theory (EFT) framework
  - $$\mathcal{L}_{SM} \to \mathcal{L}_{SM} + \underbrace{\sum_{i=1}^{n} \frac{c_i^{(6)}}{\Lambda^2} O_i^{(6)}}_{\text{diboson production}} + \underbrace{\sum_{i=1}^{n} \frac{c_i^{(8)}}{\Lambda^2} O_i^{(8)}}_{\text{EW diboson production (VBS)}} + \cdots$$

A. Denner, T. Hahn, Nucl. Phys. B525 (1998) 27-50

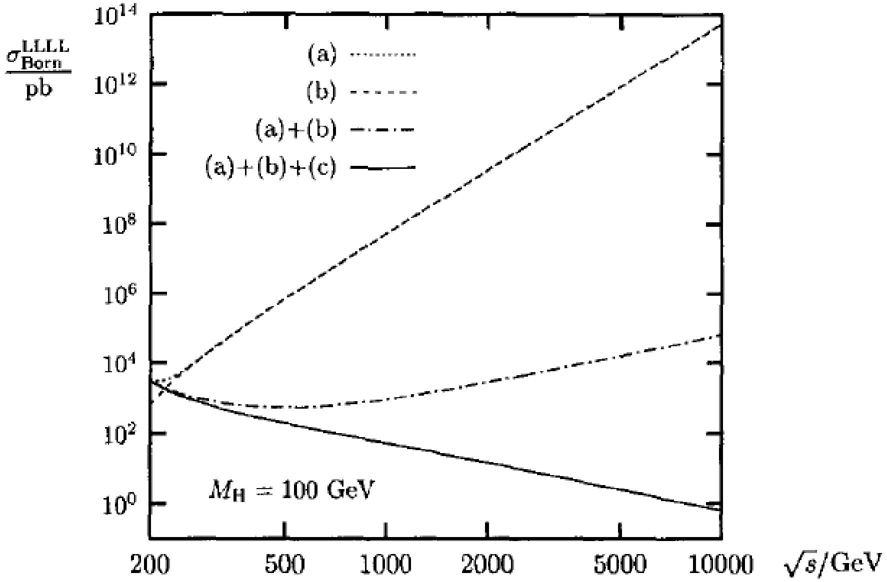

(a) 3-point gauge couplings

(b) 4-point gauge couplings

(c) couplings involving the Higgs

Precise measurements at the LHC

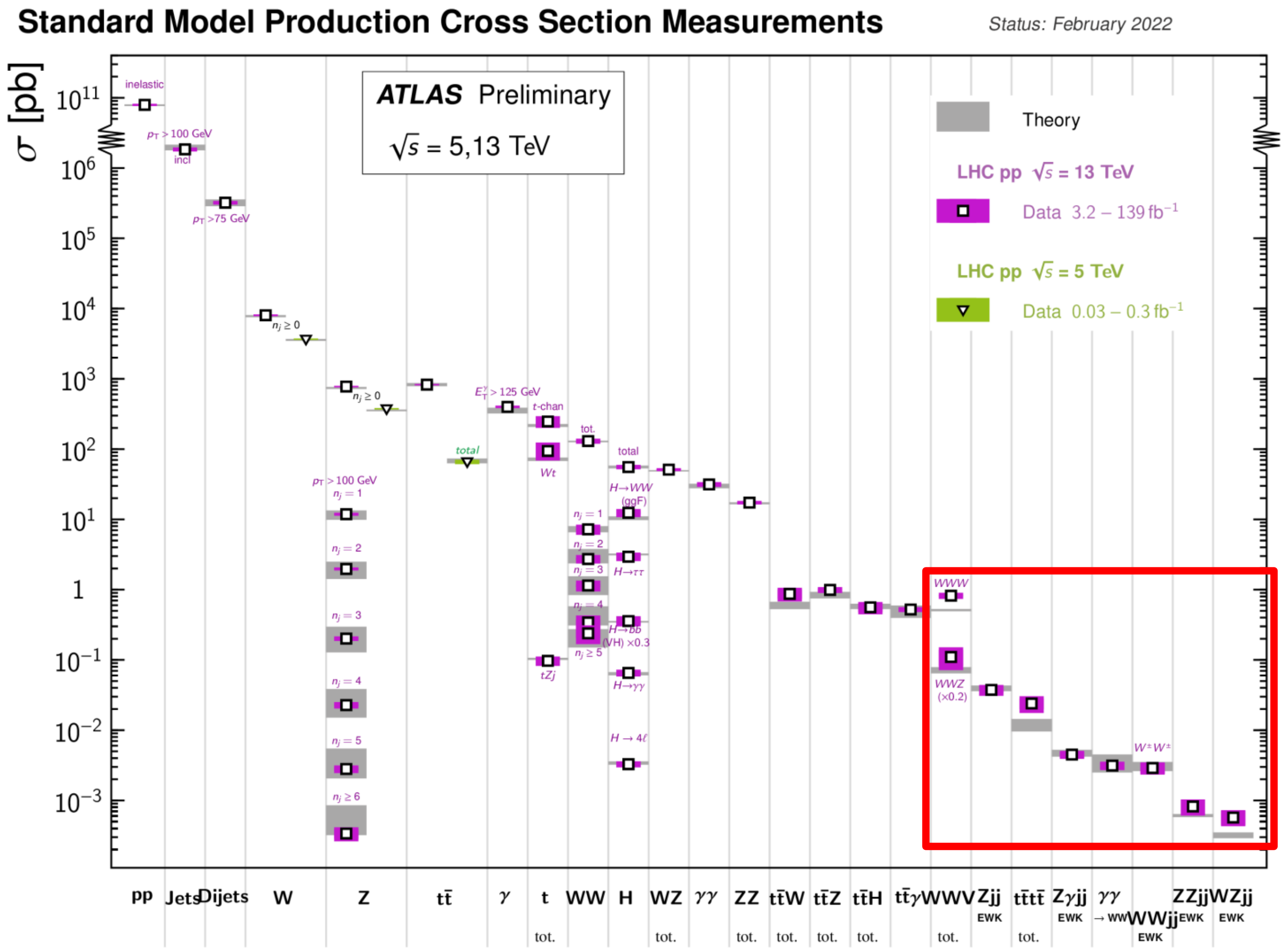

A large number of QCD/EW processes have been measured at the LHC with remarkable agreement with the Standard Model (SM) predictions over many orders of magnitude

- Vector boson scattering (VBS) processes
- Triboson production

→ Sensitive to 3-, 4-point gauge couplings

ATLAS and CMS experiments

Proton-proton collisions at the LHC started since 2010

- Run-1 (2010 – 2012): $\sqrt{s} = 7$ TeV (5 fb^{-1}), $\sqrt{s} = 8$ TeV (25 fb^{-1})
- Run-2 (2015 – 2018): $\sqrt{s} = 13$ TeV (140 fb^{-1})
- Run-3 (2022 –): $\sqrt{s} = 13.6$ TeV (65 fb^{-1})

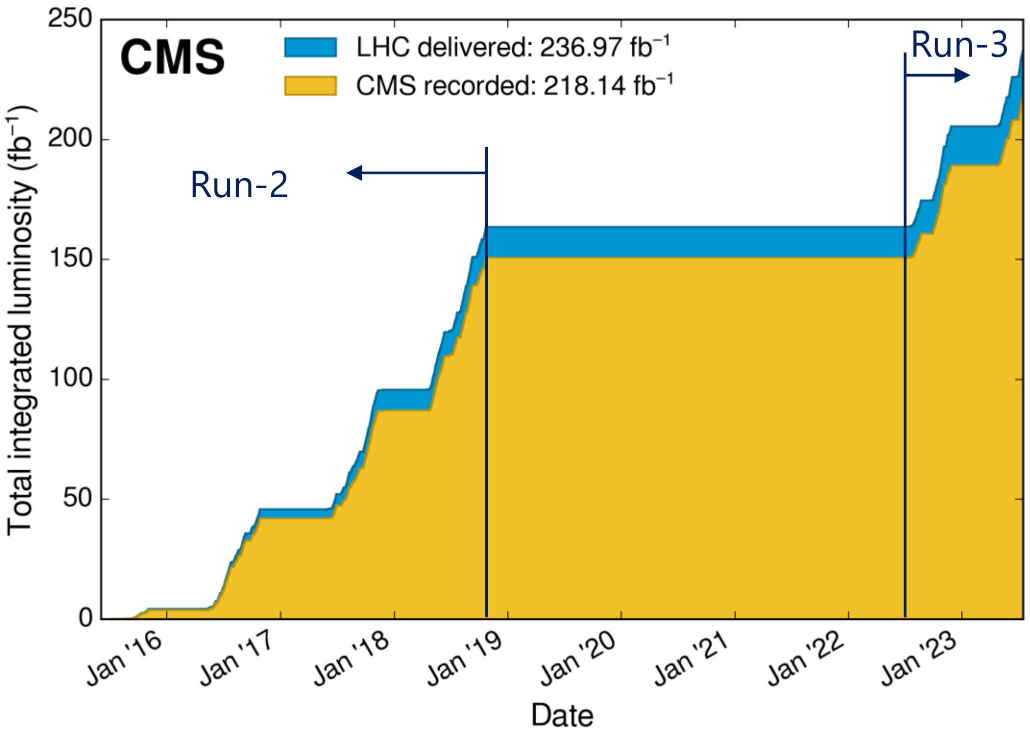

Run-2

Run-3

Pileup events/bunch crossing in Run-2

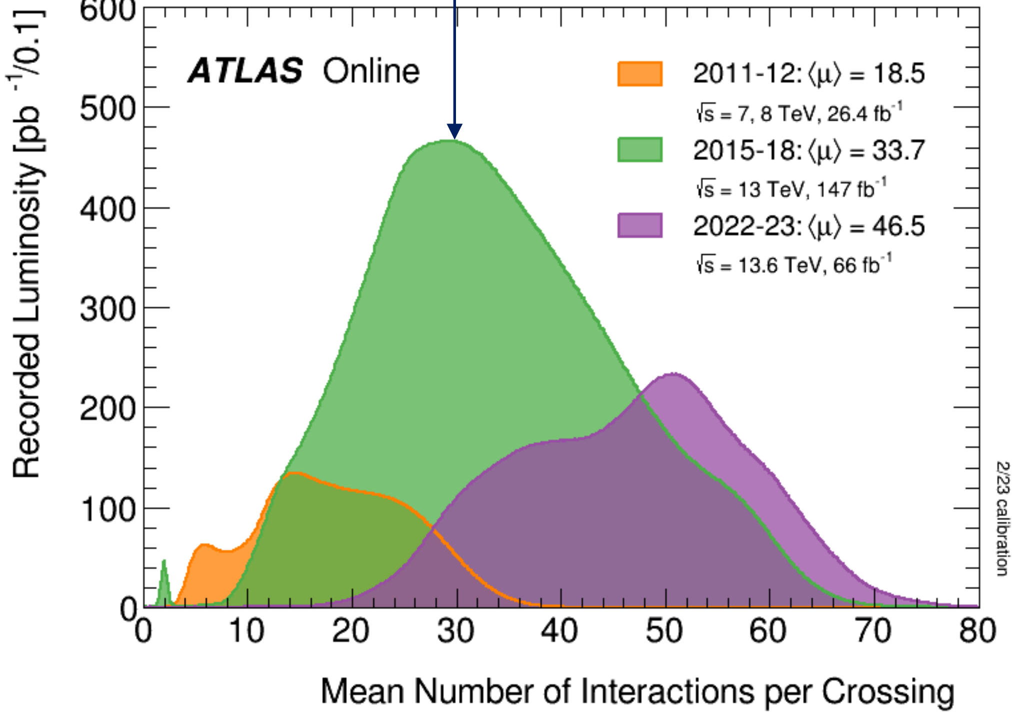

List of VBS results with full Run-2 data

Process	**ATLAS**	**CMS**
same-sign WW+jj ss$WW(\to \tau\nu)$+jj	ATLAS-CONF-2023-023	Phys. Lett. B 812 (2020) 136018 CMS-PAS-SMP-22-008
opposite-sign $WW(2l2\nu)$+jj	ATLAS-CONF-2023-039	Phys. Lett. B 841 (2023) 137495
ZZ (4l)+jj ZZ $(2l2\nu)$+jj	arXiv:2308.12324 Nat. Phys. 19, 237-253 (2023)	Phys. Lett. B 812 (2021) 135992
$W\gamma$+jj		Phys. Rev. D 108 (2023) 032017
$Z(2l)\gamma$+jj $Z(2\nu)\gamma$+jj	arXiv:2305.19142 JHEP 06 (2023) 082	Phys. Rev. D 104 (2021) 072001
WV+jj semileptonic		Phys. Lett. B 834 (2022) 137438
$WW + WZ$ combination	ATLAS-PHYS-PUB-2023-002	
$\gamma\gamma \to WW$	Phys. Lett. B 816 (2021) 136190	
$\gamma\gamma \to VV$ fully hadronic		JHEP 07 (2023) 229

List of triboson results

Process	**ATLAS**	**CMS**
$W\gamma\gamma$	arXiv:2308.03041	JHEP 10 (2021) 174
$Z\gamma\gamma$	Eur. Phys. J C 83 (2023) 539	
$WW\gamma$ $WZ\gamma$	arXiv:2305.16994	Phys. Rev. D 90 (2014) 032008
WWW	Phys. Rev. Lett. 129 (2022) 061803	Phys. Rev. Lett. 125 (2020) 151802
VVV(multi-leptons)		

VBS diagrams

$$pp \rightarrow VV + jj \rightarrow (f\bar{f})(f\bar{f}) + jj$$

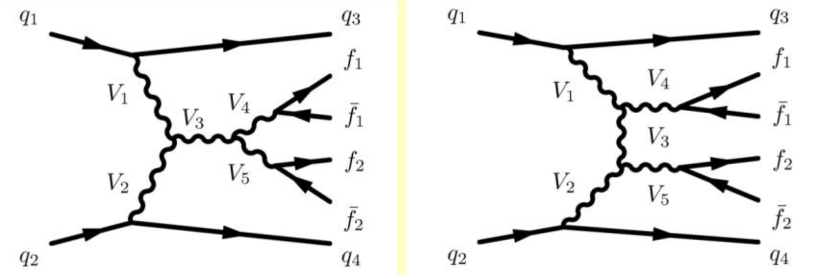

Triple gauge couplings (TGC)

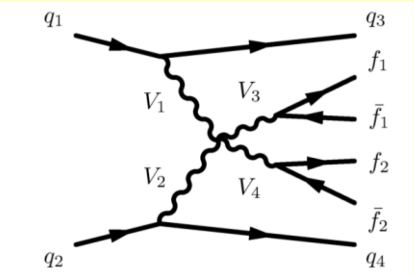

Quartic gauge couplings (QGC)

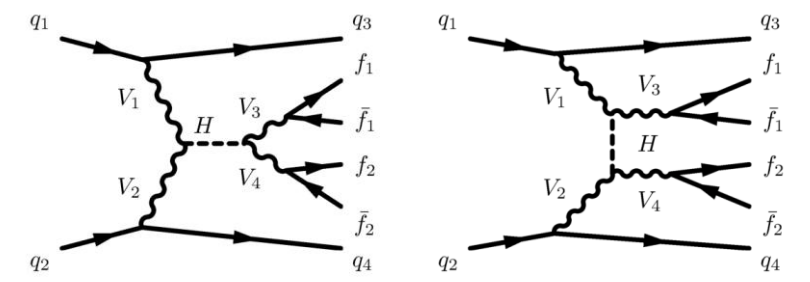

Higgs couplings

VBS diagrams

Final states with the decay products of the bosons and two forward jets are used to enhance VBS-type contributions

Non-VBS diagrams

EW

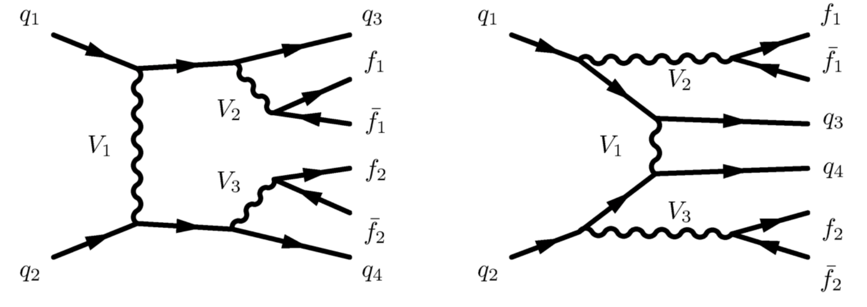

QCD

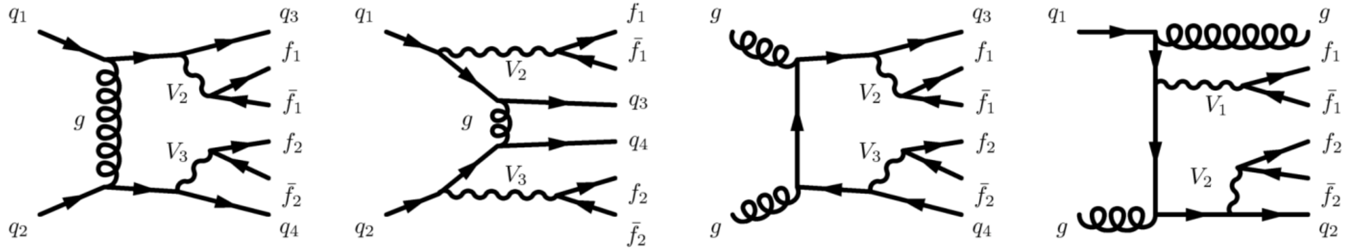

Same-sign WW production by ATLAS

ATLAS-CONF-2023-23

- Same-sign $W^{\pm}W^{\pm}$ is the most efficient channel to suppress the QCD production of VV initiated by quarks and gluons
- Largest systematics:
  - modelling of QCD correction to EW $W^{+}W^{-}$jj

Event selection

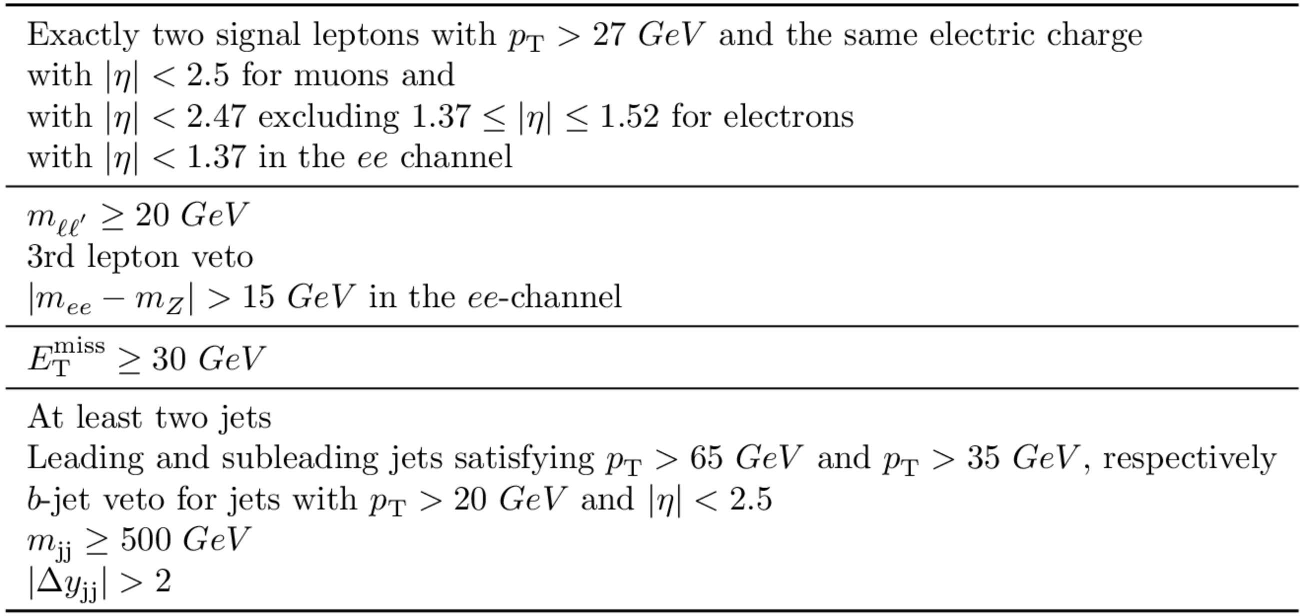

Exactly two signal leptons with $p_{\mathrm{T}} > 27\ GeV$ and the same electric charge with $\lvert\eta\rvert < 2.5$ for muons and with $\lvert\eta\rvert < 2.47$ excluding $1.37 \leq \lvert\eta\rvert \leq 1.52$ for electrons with $\lvert\eta\rvert < 1.37$ in the ee channel
$m_{\ell\ell'} \geq 20\ GeV$ 3rd lepton veto $\lvert m_{ee} - m_Z\rvert > 15\ GeV$ in the ee-channel
$E_{\mathrm{T}}^{\mathrm{miss}} \geq 30\ GeV$
At least two jets Leading and subleading jets satisfying $p_{\mathrm{T}} > 65\ GeV$ and $p_{\mathrm{T}} > 35\ GeV$, respectively b-jet veto for jets with $p_{\mathrm{T}} > 20\ GeV$ and $\lvert\eta\rvert < 2.5$ $m_{\mathrm{jj}} \geq 500\ GeV$ $\lvert\Delta y_{\mathrm{jj}}\rvert > 2$

$$pp \to W^{\pm}W^{\pm} + jj \to l^{\pm}l^{\pm}\nu\nu + jj$$

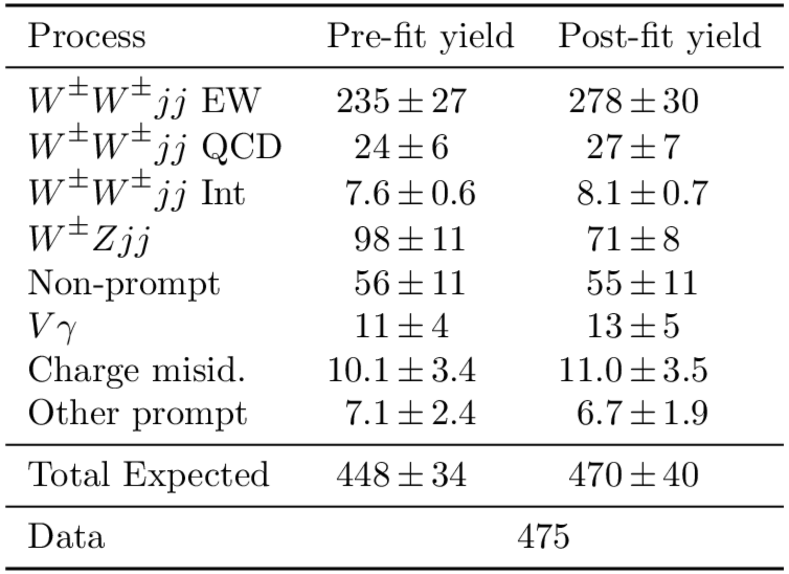

Process	Pre-fit yield	Post-fit yield
$W^{\pm}W^{\pm}jj$ EW	235 ± 27	278 ± 30
$W^{\pm}W^{\pm}jj$ QCD	24 ± 6	27 ± 7
$W^{\pm}W^{\pm}jj$ Int	7.6 ± 0.6	8.1 ± 0.7
$W^{\pm}Zjj$	98 ± 11	71 ± 8
Non-prompt	56 ± 11	55 ± 11
$V\gamma$	11 ± 4	13 ± 5
Charge misid.	10.1 ± 3.4	11.0 ± 3.5
Other prompt	7.1 ± 2.4	6.7 ± 1.9
Total Expected	448 ± 34	470 ± 40
Data	475	

Fiducial cross section

$$\sigma_{\mathrm{fid}}^{\mathrm{EW}} = 2.88 \pm 0.21(\mathrm{stat.}) \pm 0.19(\mathrm{syst.})\ \mathrm{fb}$$

Same-sign WW differential cross sections

ATLAS-CONF-2023-23

- Extracted the differential cross sections vs. $m_{ll}, m_T, m_{jj},\ N_{\text{gap jets}}, \xi_{j3}$
- Good agreements with SM predictions in general (MG+Herwig, MG+Pythia, Sherpa (NLO))
  - Some mismodelling in the cross section against m_T
  - Data tend to underestimate the predictions and the NLO calculation gives slightly lower predictions to others

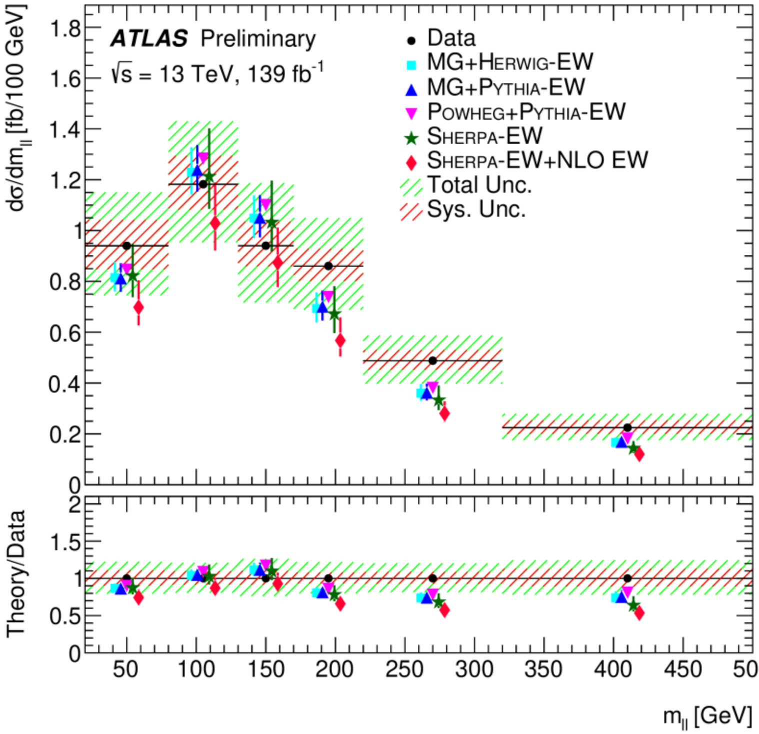

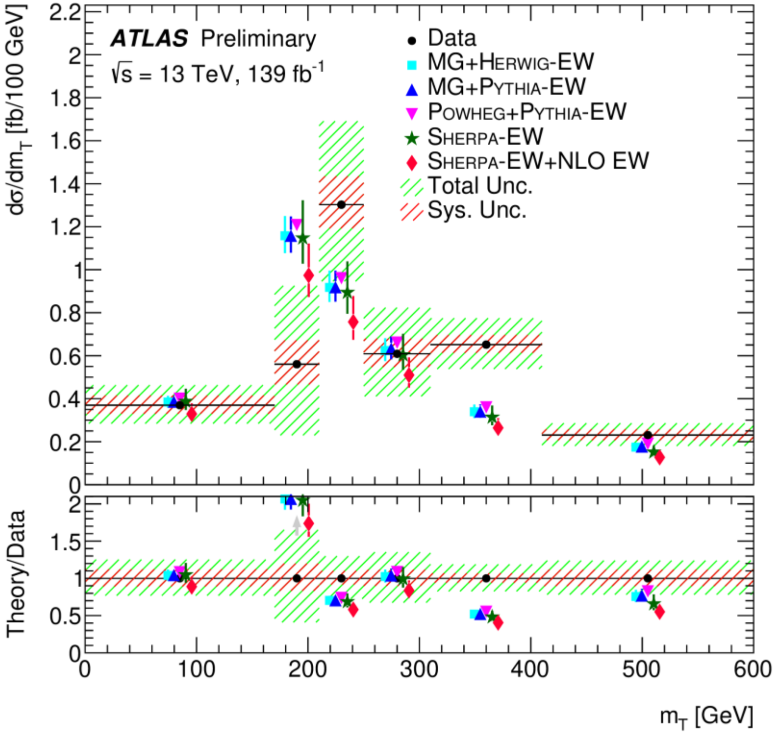

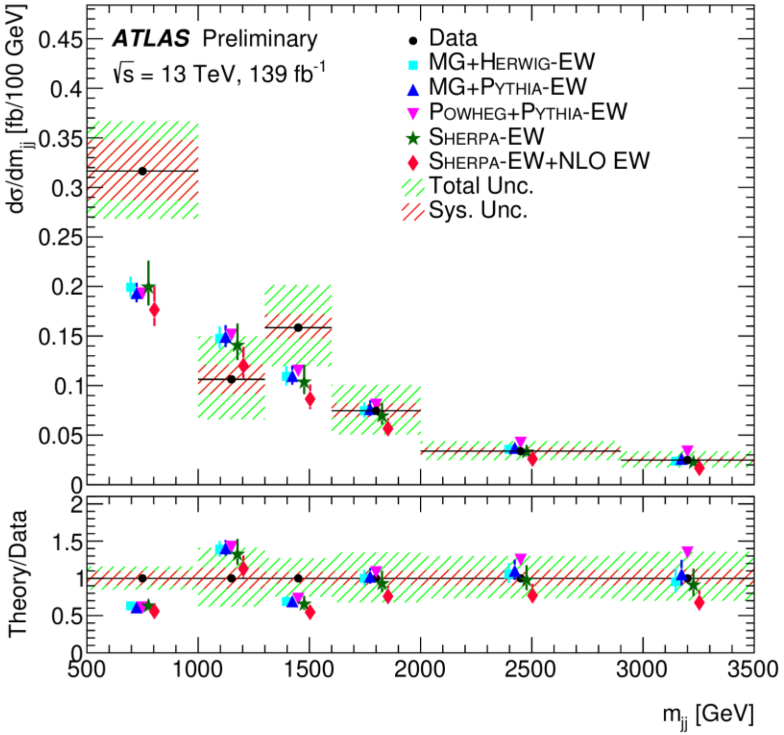

EFT interpretation of the same-sign WW results

Same-sign WW cross sections are used to constrain the dimension-8 operator coefficients

$$\mathcal{L}_{\text{eff}} = \mathcal{L}_{\text{SM}} + \sum_i \frac{f_i^{(6)}}{\Lambda^2} O_i^{(6)} + \sum_j \frac{f_j^{(8)}}{\Lambda^4} O_j^{(8)} + \dots$$

Dimension-8 operators (Eboli model):

- Scalar terms (only Φ)
- Tensor terms (only $W^{\mu\nu}$ and $B^{\mu\nu}$)
- Mixed terms (mix of Φ, $W^{\mu\nu}$ and $B^{\mu\nu}$)

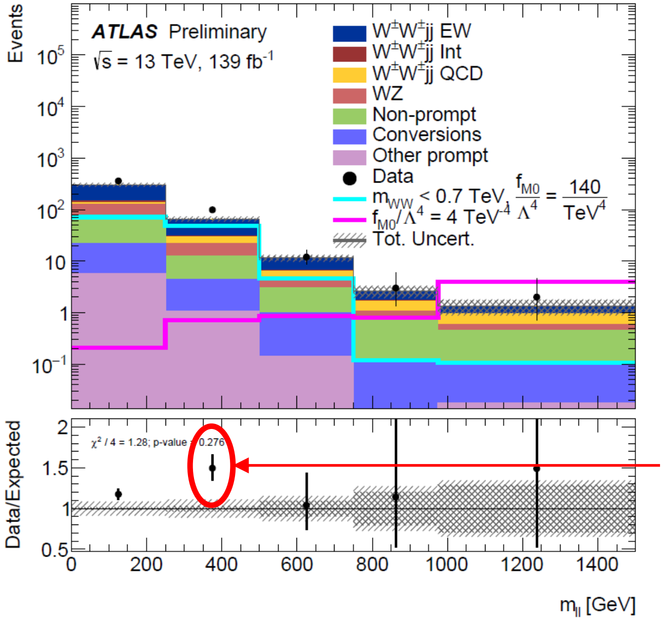

- Fit the m_{ll} distribution with the EFT model with 1 or 2 free parameter(s) at a time
- Limits are extracted by evaluating both the experimental limits and the theoretical unitarity bounds
- Excess of events at m_{ll}~400 GeV makes the fit favor $|f_i/\Lambda^2| > 0$

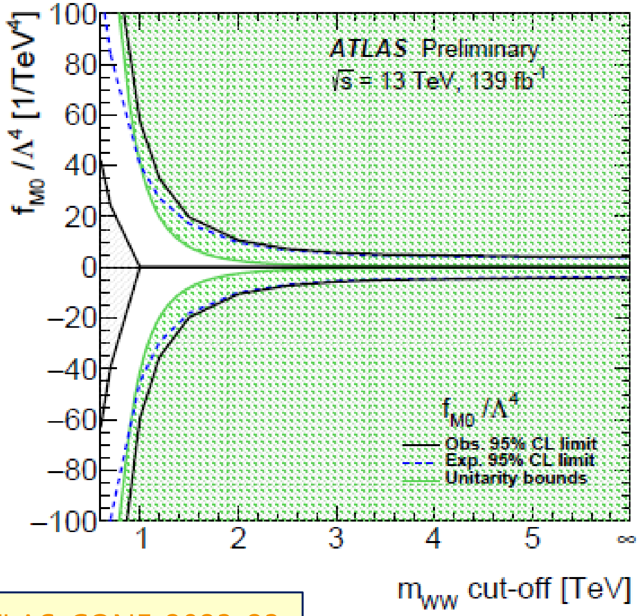

ATLAS-CONF-2023-23

Limits on the EFT coefficients

- Limits on the dimension-8 coefficients (f_i/Λ^2) at 95% C.L. are obtained and correlations of pair in the same type are shown (SM value is at the origin)
- The effect of the unitarization are also shown

ATLAS-CONF-2023-23

Cut-off scale: 1.5 TeV

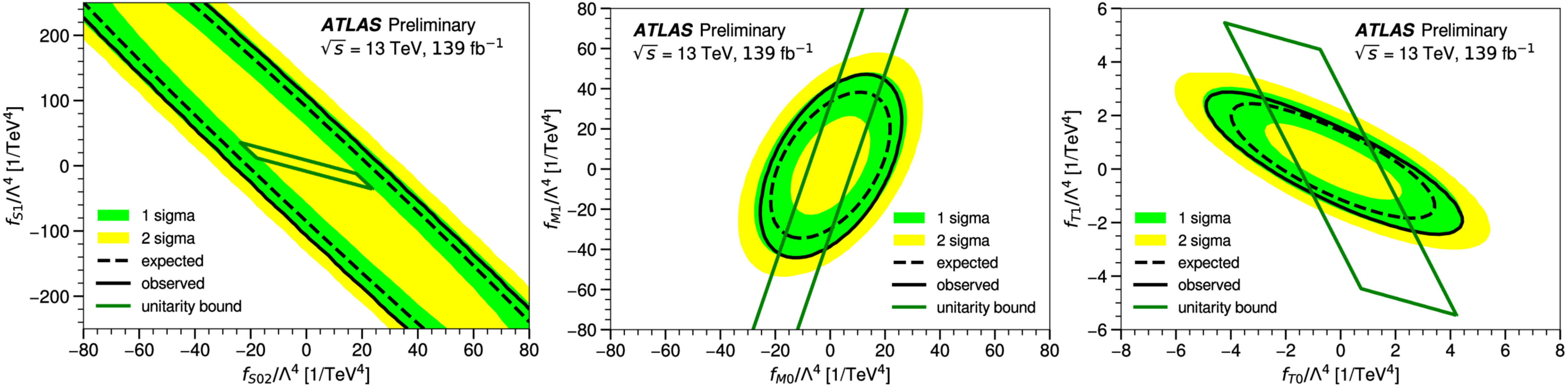

Same-sign WW measurement by CMS

- $W^{\pm}W^{\pm}+jj \rightarrow l^{\pm}l^{\pm}\nu\nu+jj$ mode
- Use a Boosted Decision Tree (BDT) to separate
  - $W_L W_L$ against $W_T W_X$ or
  - $W_L W_X$ against $W_T W_T$
- Cross sections for each polarization combination are extracted

Variables used in the BDT:

- $m_{jj}, |\Delta\eta_{jj}|, \Delta\phi_{jj}, \Delta\phi_{ll}, p_T^{ll}, p_T^{miss}$
- p_T of the leading/subleading jet or lepton
- $z_{l_1}^*, z_{l_2}^*$: Zeppenfeld variables for the leptons

Phys. Lett. B812 (2021) 136018

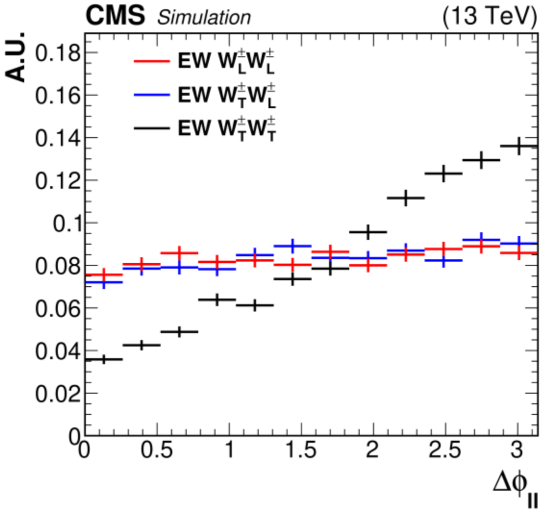

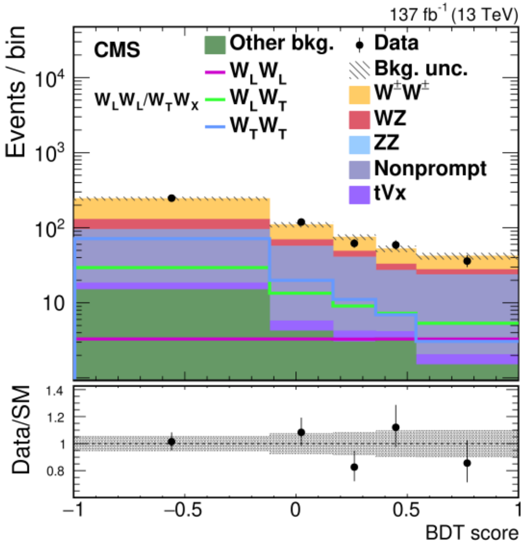

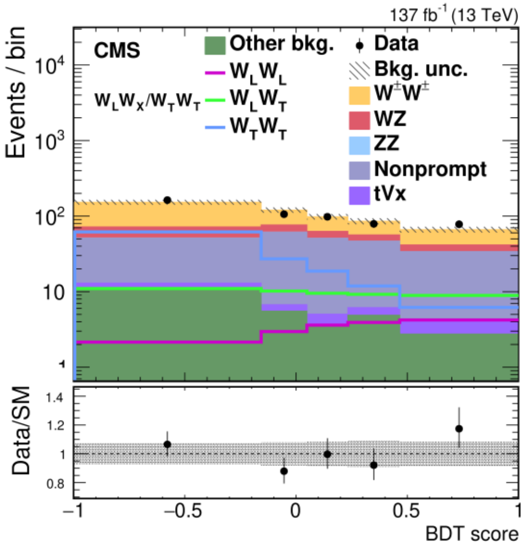

- Cross sections for each polarization combination
- Still large uncertainty for $W_L^{\pm}W_L^{\pm}$
- Helicity eigenstates are defined in the WW center-of-mass frame

Process	$\sigma\mathcal{B}$ (fb)	Theoretical prediction (fb)
$W_L^{\pm}W_L^{\pm}$	$0.32^{+0.42}_{-0.40}$	0.44 ± 0.05
$W_X^{\pm}W_T^{\pm}$	$3.06^{+0.51}_{-0.48}$	3.13 ± 0.35
$W_L^{\pm}W_X^{\pm}$	$1.20^{+0.56}_{-0.53}$	1.63 ± 0.18
$W_T^{\pm}W_T^{\pm}$	$2.11^{+0.49}_{-0.47}$	1.94 ± 0.21

EW W^+W^- production by CMS (1)

Measurement of the opposite-sign W^+W^- events produced by EW interactions is difficult due to the large backgrounds from $t\bar{t}$ and quark/gluon-initiated processes (QCD)

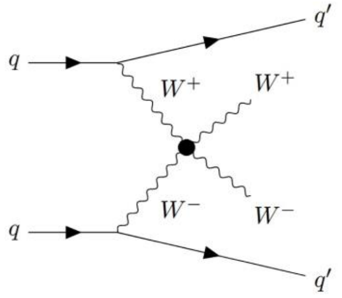

QGC

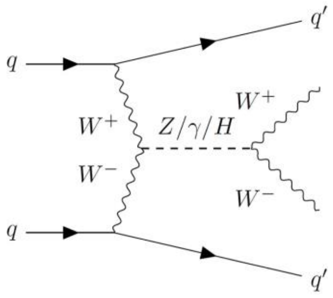

TGC

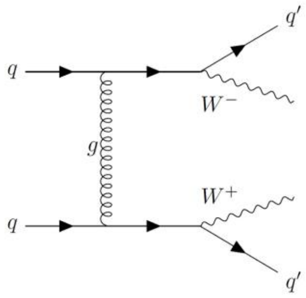

QCD

- For the $e\mu$ final state, use a deep neural network (DNN) to extract the VBS signal from the $t\bar{t}$ and QCD-induced backgrounds

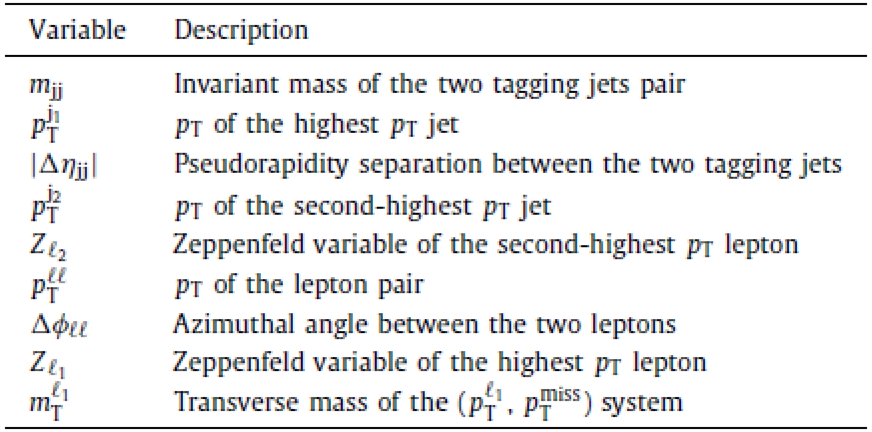

Variable	Description
m_{jj}	Invariant mass of the two tagging jets pair
$p_{\mathrm{T}}^{\mathrm{j_1}}$	p_{T} of the highest p_{T} jet
$\lvert\Delta\eta_{\mathrm{jj}}\rvert$	Pseudorapidity separation between the two tagging jets
$p_{\mathrm{T}}^{\mathrm{j_2}}$	p_{T} of the second-highest p_{T} jet
Z_{ℓ_2}	Zeppenfeld variable of the second-highest p_{T} lepton
$p_{\mathrm{T}}^{\ell\ell}$	p_{T} of the lepton pair
$\Delta\phi_{\ell\ell}$	Azimuthal angle between the two leptons
Z_{ℓ_1}	Zeppenfeld variable of the highest p_{T} lepton
$m_{\mathrm{T}}^{\ell_1}$	Transverse mass of the $(p_{\mathrm{T}}^{\ell_1}, p_{\mathrm{T}}^{\mathrm{miss}})$ system

$e\mu$ channel (SR)

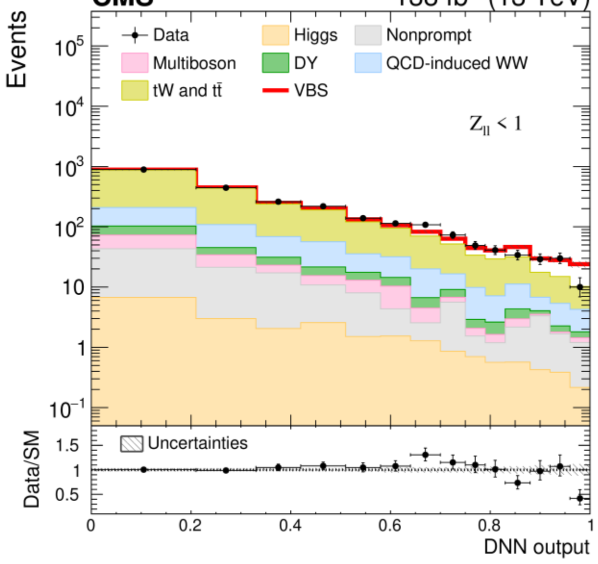

$e\mu$ channel (CR)

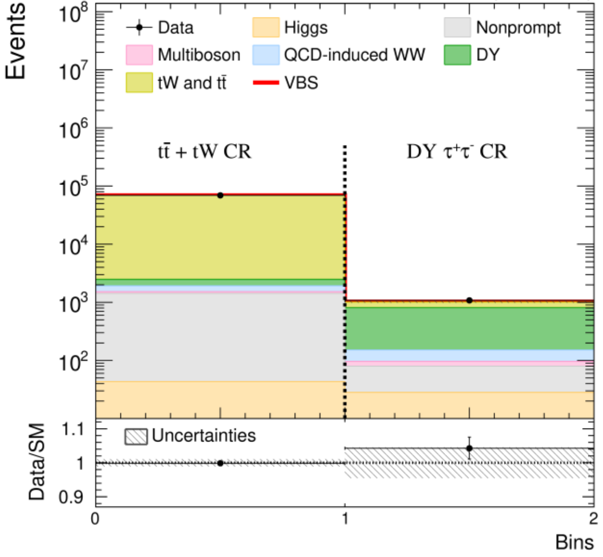

Phys. Lett. B841 (2023) 137495

EW W^+W^- production by CMS (2)

$ee/\mu\mu$ channel (Signal region)

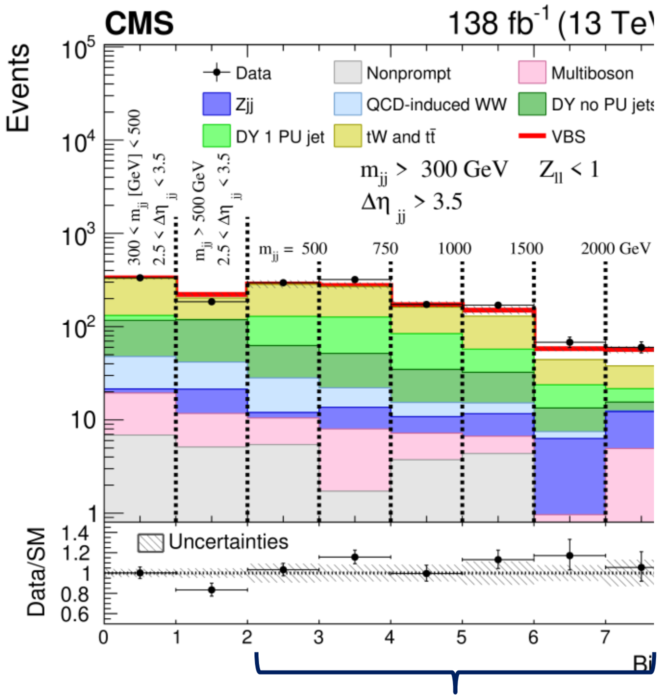

m_{jj} distribution

$ee/\mu\mu$ channel (Control region)

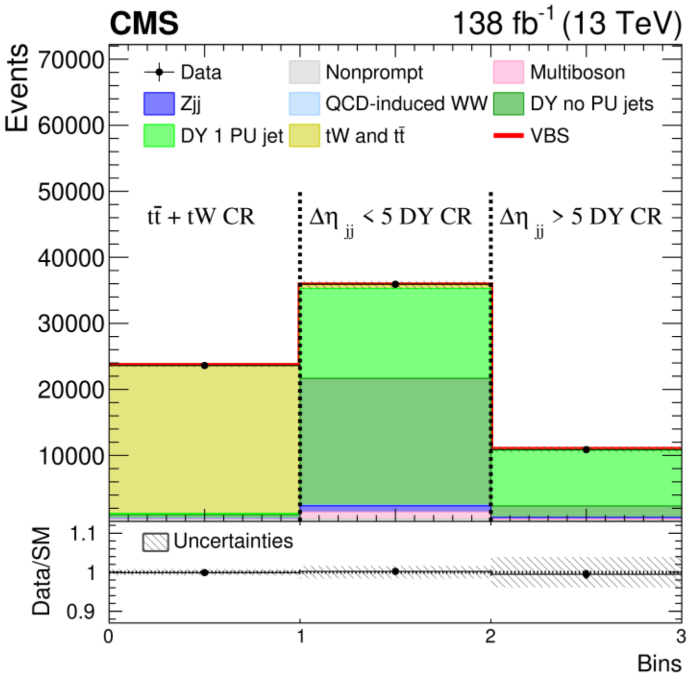

- Discriminating variables:
  - number of events in the 8 signal regions ($ee/\mu\mu$)
  - DNN output ($e\mu$)
- Fit all discriminating variables including the number of events in the control regions (CRs) with $\mu_{EW} = \sigma_{obs}/\sigma_{SM}$ as the parameter

Cross section:

- 99 ± 20 fb (89 ± 5 fb expected)
- $5.6\ (5.2)\sigma$ observed (expected) significance

EW $W^{+}W^{-}$ production by ATLAS

The ATLAS experiment has also conducted the measurement of $pp \rightarrow W^{+}W^{-} + jj \rightarrow e\mu + \nu\nu + jj$

- Use events with 2 or 3 jets
- Neural network is used to extract the signal
  - Background: $t\bar{t}$, QCD-induced $W^{+}W^{-}$

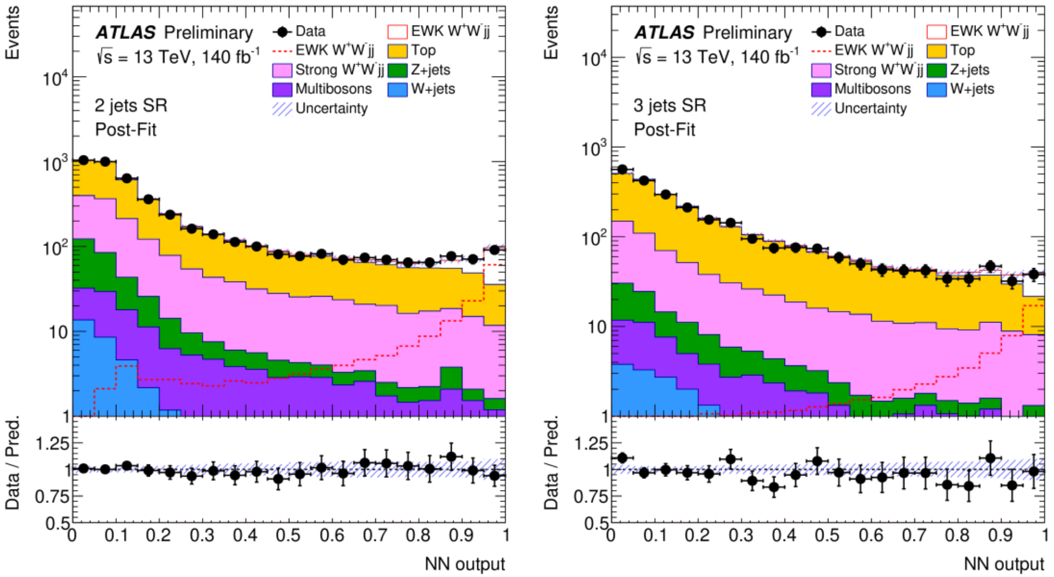

ATLAS-CONF-2023-039

Process	Event yields $n_{\text{jets}} = 2$	$n_{\text{jets}} = 3$
EWK $W^{+}W^{-}jj$	158 ± 27	54 ± 13
Top quark	2885 ± 214	1851 ± 131
Strong $W^{+}W^{-}jj$	1214 ± 256	514 ± 121
W+jets	37 ± 97	19 ± 48
Z+jets	216 ± 62	65 ± 25
Multiboson	101 ± 5	42 ± 3
SM prediction	4610 ± 77	2546 ± 48
Data	4610	2533

Signal strengths

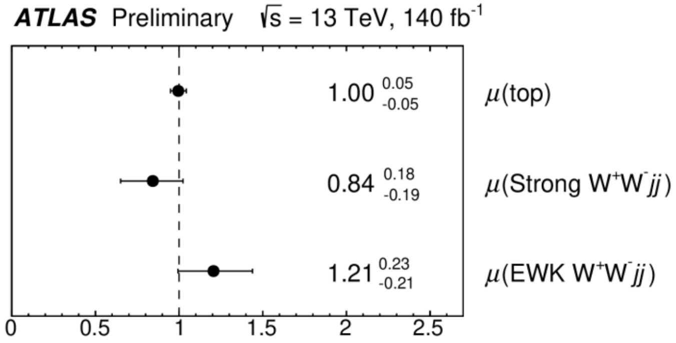

Combined fit of the NN output in SRs and CRs using signal strength (μ) and the normalization of $t\bar{t}$ and QCD backgrounds as parameters (3 parameters)

- Significance: 7.1 observed (6.2σ expected)
- $2.65^{+0.52}_{-0.48}$ fb (observed)
- $2.20^{+0.14}_{-0.13}$ fb (Powheg Boxv2)

VBS in semileptonic mode (1)

Phys. Lett. B34 (2022) 137438

- Semileptonic channels of $W+W/Z$ (CMS)
  - larger branching ratios
  - larger background ($t\bar{t}$, W+jets)
- Use DNN to separate signal from the large background
- First results in the semileptonic mode

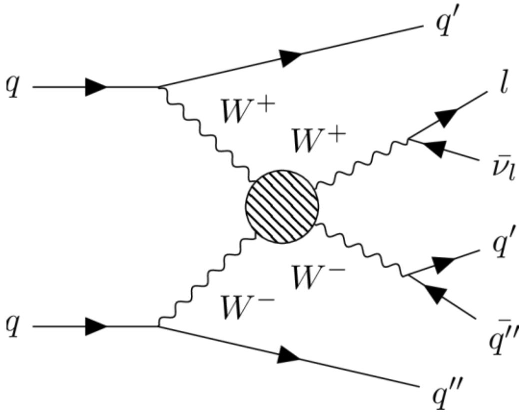

Reconstructed as either two jets (jj) or one large-R jet (J)

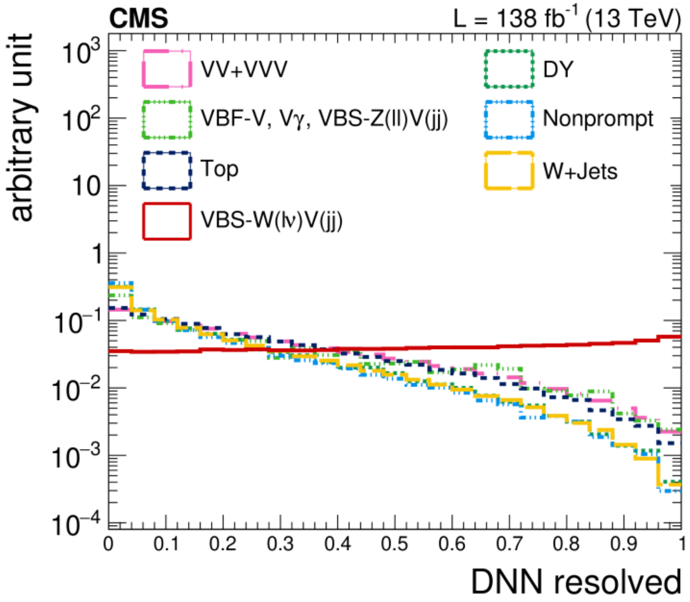

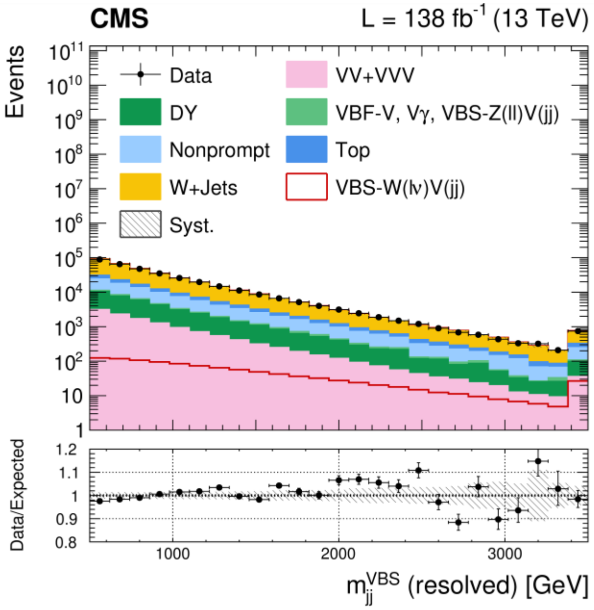

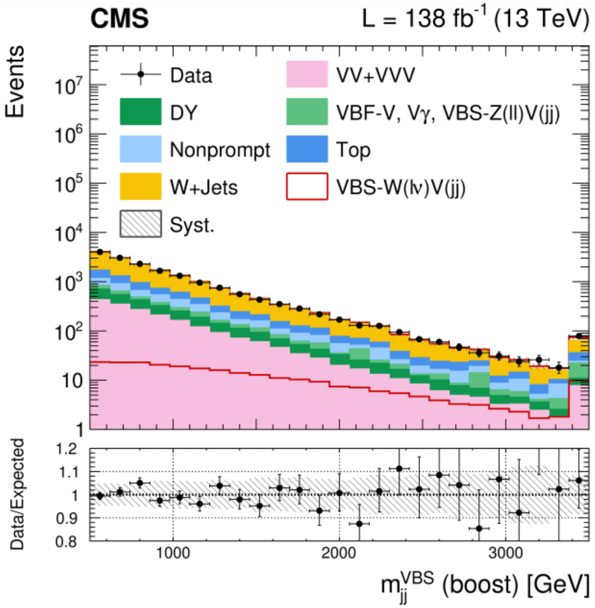

VBS in semileptonic mode (2)

Phys. Lett. B34 (2022) 137438

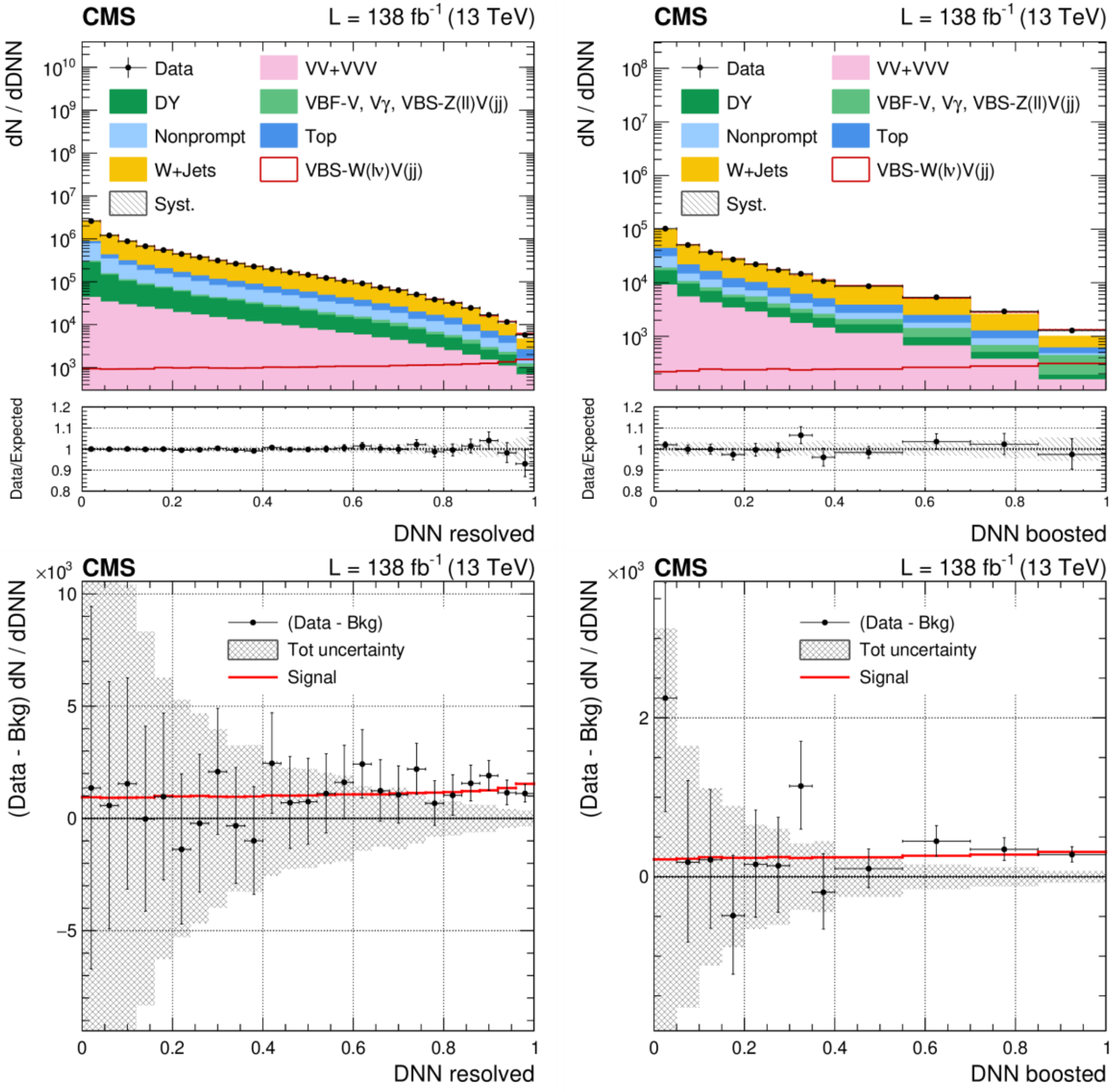

EW-only fit ($\mu_{\mathrm{QCD}} = 1$)

- $\mu_{\mathrm{EW}} = \frac{\sigma^{\mathrm{obs}}}{\sigma^{\mathrm{SM}}} = 0.85 \pm 0.12(\mathrm{stat})^{+0.19}_{-0.17} = 0.85^{+0.23}_{-0.21}$
- 4.4σ (observed), 5.1σ (expected)
- $1.90^{+0.53}_{-0.46}$ pb (observed)

2 parameter fit with μ_{EW} and μ_{QCD} correlation

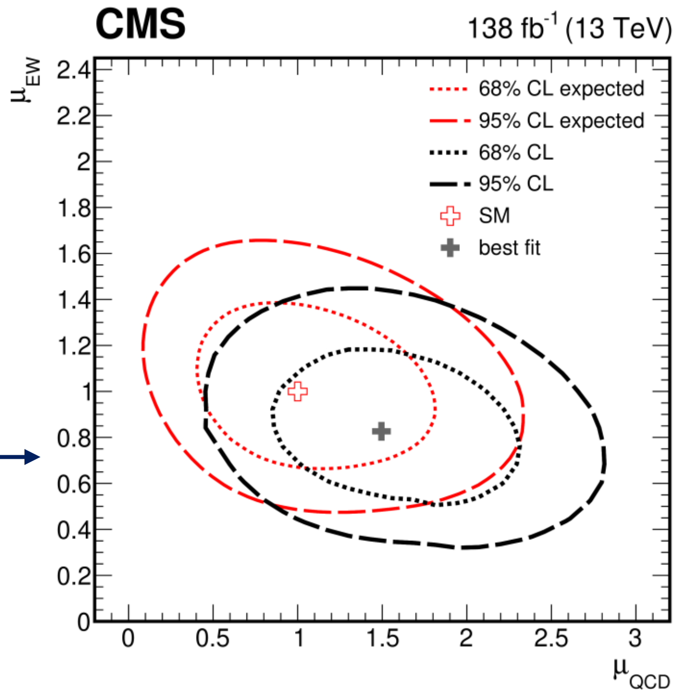

Differential cross section of $pp \rightarrow ZZ(4l) + jj$

arxiv:2308.12324

- $pp \rightarrow ZZ + jj$ in the 4 lepton final state by ATLAS
  - Both EW/QCD productions are important to fully understand the production mechanism
- Differential cross sections
  - VBS observables ($m_{4l}, p_{T,4l}, m_{jj}, |\Delta y_{jj}|, p_{T,jj}$)
  - Polarization, charge conjugation and parity observables
    - $\cos\theta^*_{12}, \cos\theta^*_{34}$ (cosine of the negatively-charge lepton in the leading/subleading Z boson frame)
    - $\Delta\phi_{jj} = \phi_f - \phi_b$ (signed azimuthal angle of the two jets)
  - QCD observables ($p_{T,4ljj}, S_{T,4ljj}$)
- Centrality of the four-lepton system ($\xi = \left|\frac{y_{4l} - 0.5(y_{j_1} - y_{j_2})}{\Delta y_{jj}}\right|$)
  - $\xi < 0.4$ (VBS-enhanced), $\xi > 0.4$ (VBS-suppressed)

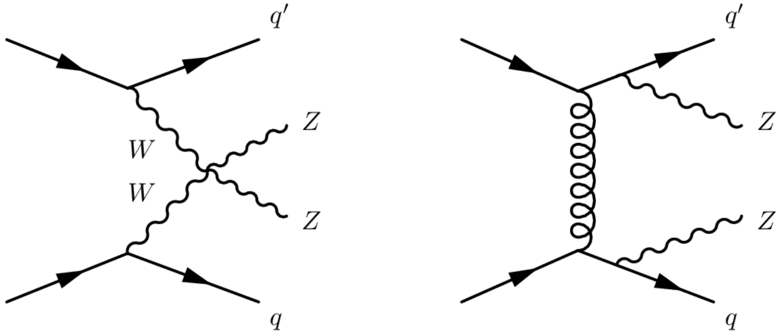

Process	Event yield ± stat. ± syst.	
	VBS-enhanced	VBS-suppressed
strong $4\ell jj$ (SHERPA)	98.9 ± 0.5 ± 25.2	45.5 ± 0.3 ± 12.9
EW $4\ell jj$ (MG5+PY8)	24.1 ± 0.1 ± 1.8	2.12 ± 0.02 ± 0.14
Prompt background	18.8 ± 0.2 ± 2.2	5.5 ± 0.1 ± 0.4
Non-prompt background	3.0 ± 0.6 ± 3.2	1.1 ± 0.5 ± 1.2
Total prediction	144 ± 1 ± 26	54 ± 1 ± 13
Data	169	53

$ZZ(4l) + jj$ differential cross section results

- $ZZ(\rightarrow 4l) + jj$ differential cross sections in the VBS-enhanced SR
- Good agreement of cross sections with SHERPA (although larger theoretical uncertainties)
- MG5+Pythia8 underestimates the inclusive $4ljj$ cross section in all distributions
- Limits on dimension-8 coefficients in EFT are also obtained

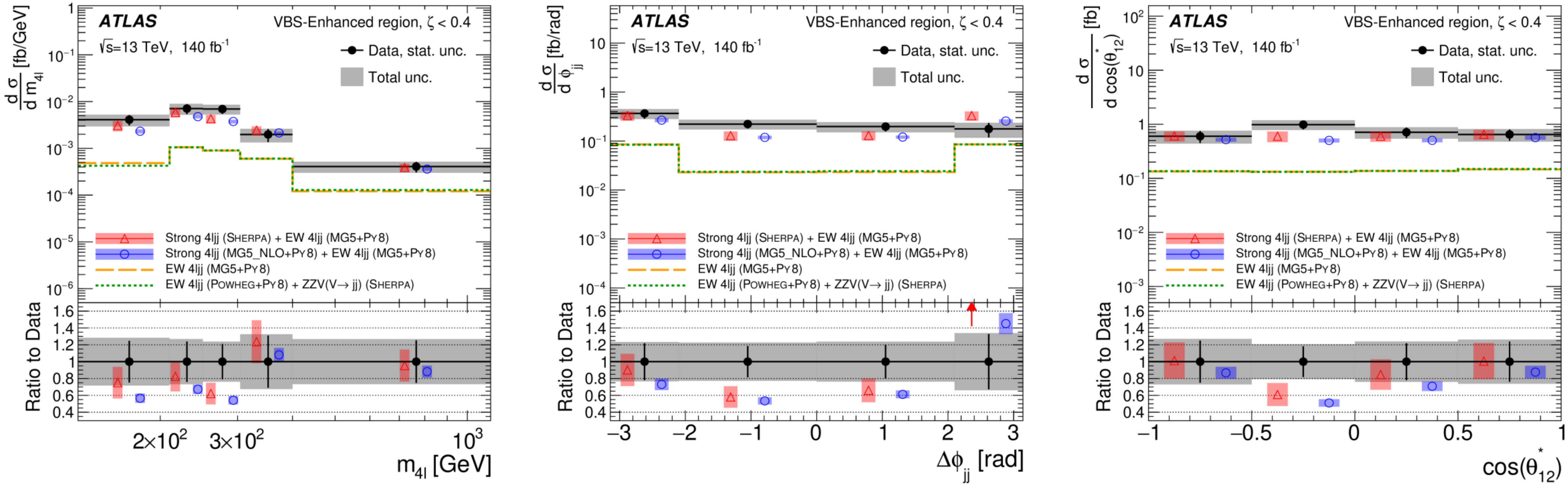

High-mass exclusive $\gamma\gamma \to VV$ production (1)

CMS+TOTEM, JHEP 07 (2023) 229

- Scattering of two photons radiated by the protons at small angles
- Forward proton tag
  - Precision Proton Spectrometer (PPS) located around 200 m from the interaction point. PPS consists of Roman pots
  - Fractional momentum loss: $0.04 < \xi < 0.20$
- Physics process
  - High-mass $\gamma\gamma \to WW, \gamma\gamma \to ZZ$
  - Full $pWWp$ or $pZZp$ system can be reconstructed by PPS and the central CMS detector
- Dataset: $\sqrt{s} = 13$ TeV, 100 fb^{-1} (2016—2018)

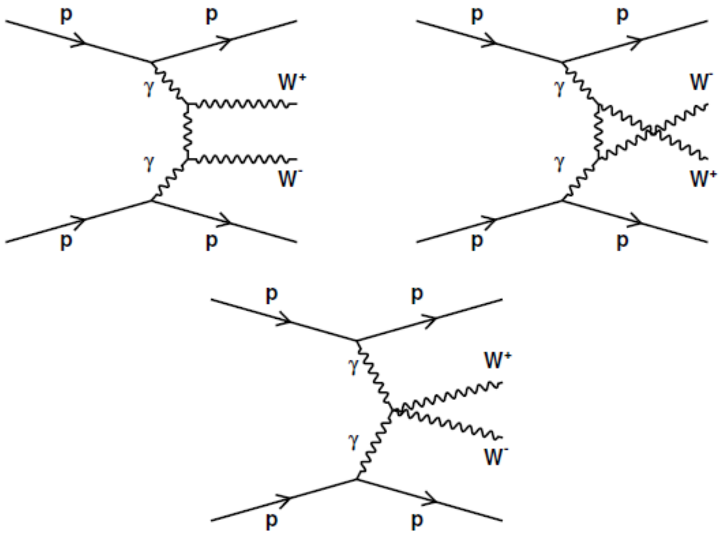

Fractional momentum loss

$$\xi = \frac{p_{\text{nom}} - p}{p_{\text{nom}}}$$

protons with a small loss of momenta

PPS

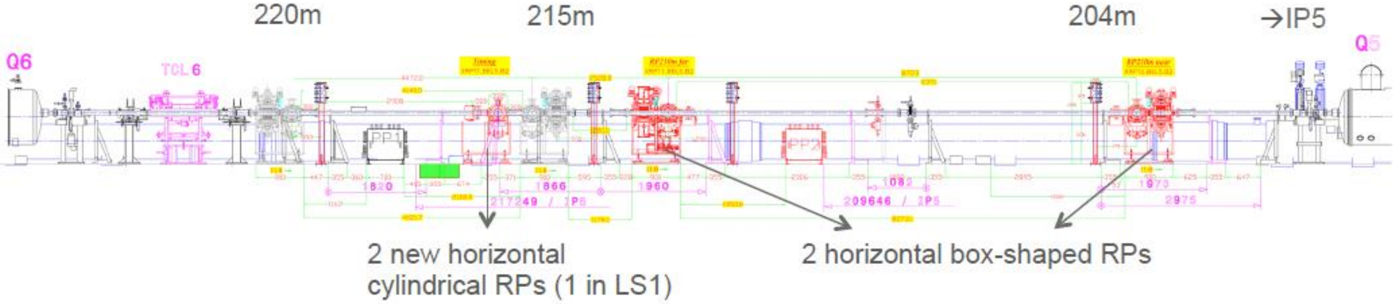

2 new horizontal cylindrical RPs (1 in LS1)

2 horizontal box-shaped RPs

High-mass exclusive $\gamma\gamma \rightarrow VV$ production (2)

- Two highest p_T jets with p_T>200 GeV, $|\eta| < 2.5$, anti-k_t jet ($R = 0.8$)
- $m(jj)$>1126 GeV, $|\Delta\eta(jj)| < 1.3$, acoplanarity<0.01, $p_T(\mathrm{j1})/p_T(\mathrm{j2}) < 1.3$
- Subjetstructure to select boosted $Z \rightarrow jj$ and $W \rightarrow jj$
    - Pruned jet mass between 60 and 107 GeV
    - Subjettiness variable: $\tau_{21} < 0.75$
    - → 85% signal efficiency, rejects 65% of QCD multijet (simulation)

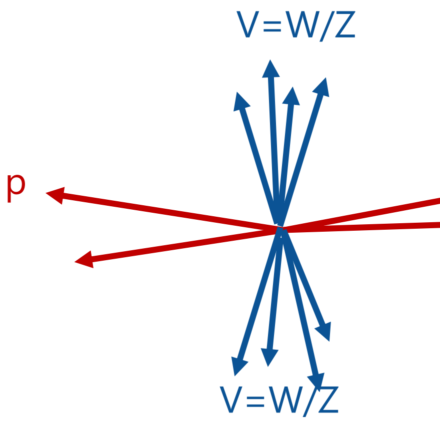

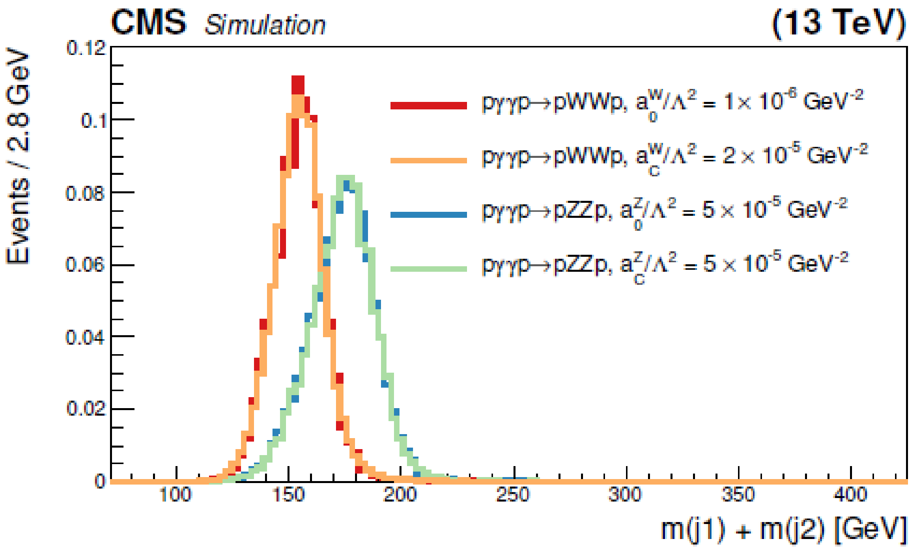

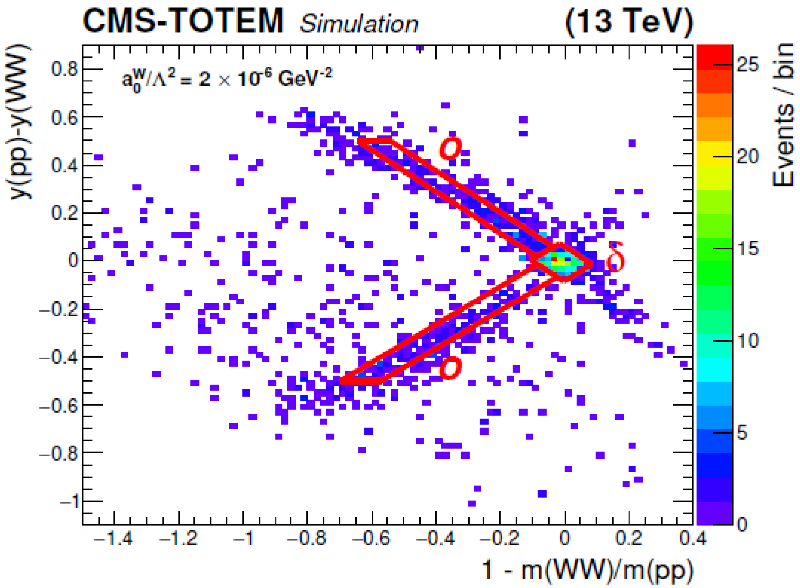

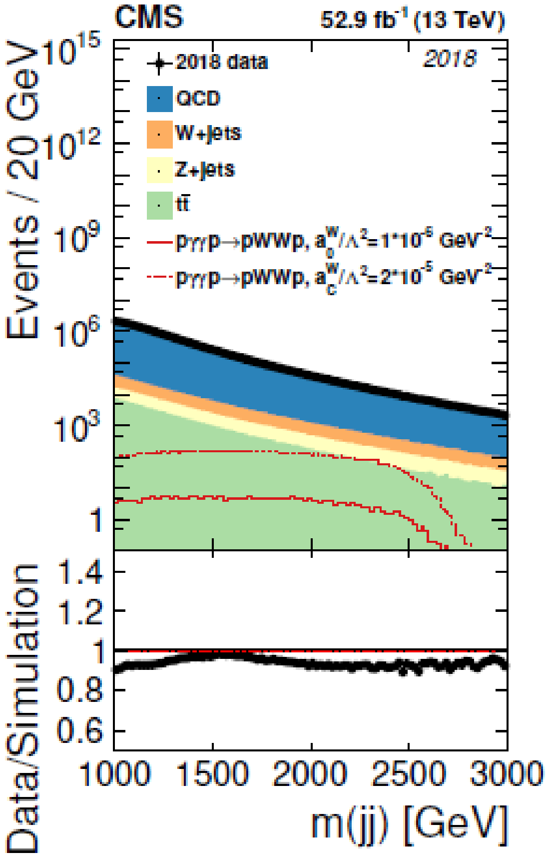

High-mass exclusive $\gamma\gamma \to VV$ production (3)

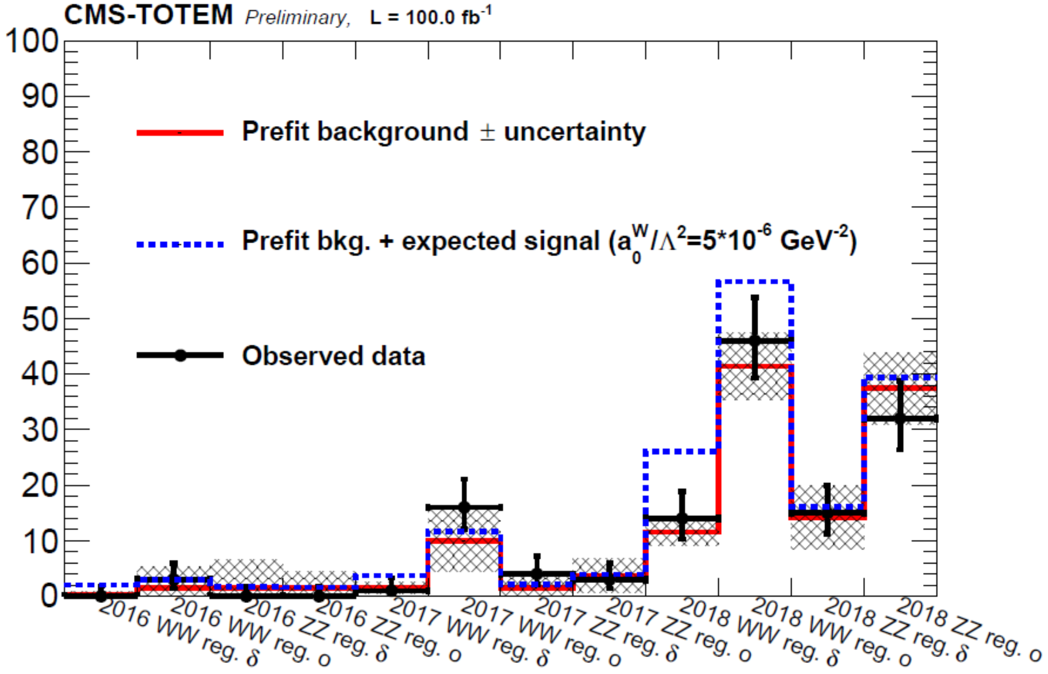

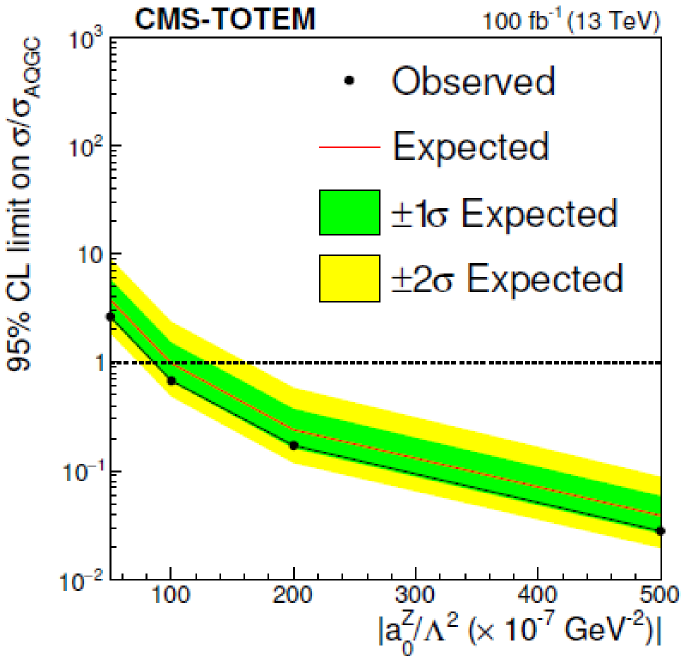

Fiducial cross section

- 0.04<ξ<0.20, $m(VV) > 1$ TeV
- $\sigma(pp \to pWWp) < 67(53^{+34}_{-19})$ fb
- $\sigma(pp \to pZZp) < 43(62^{+33}_{-20})$ fb

( ): expected value and uncertainty

Translating the limits to the dim-8 operator coefficients

Coupling	Observed (expected) 95% CL upper limit No clipping	Observed (expected) 95% CL upper limit Clipping at 1.4 TeV
$\lvert f_{M,0}/\Lambda^4\rvert$	16.2 (14.7) TeV^{-4}	19.5 (19.2) TeV^{-4}
$\lvert f_{M,4}/\Lambda^4\rvert$	90.9 (82.6) TeV^{-4}	110 (108) TeV^{-4}

$W\gamma\gamma$ cross section (ATLAS)

- Triple gauge boson production processes are also sensitive to triple- and quartic-gauge boson couplings

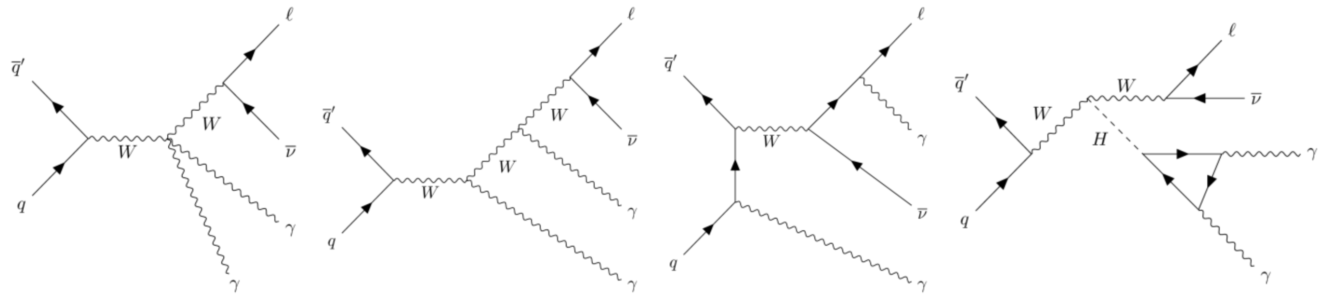

Fiducial region

- At least wo photon: p_T>20 GeV, $|\eta| < 2.37$
- Electron or muon: p_T>25 GeV, $|\eta| < 2.47$
- Isolated photons and leptons
- $\Delta R_{\gamma\gamma} > 0.4, \Delta R_{l\gamma} > 0.4$
- B-jet veto for p_T^{jet}>20 GeV, $|\eta| < 2.5$
- E_T^{miss}>25 GeV, m_T^W>40 GeV

arXiv:2308.03041

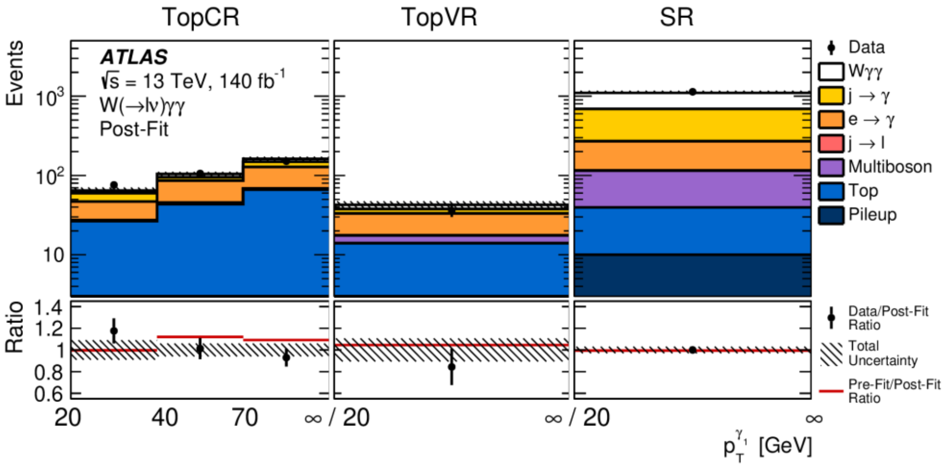

- Main backgrounds
  - fake photons from jets
  - irreducible backgrounds ($t\bar{t}\gamma, WH$, ...)
- Extract the signal strength (μ) by a simultaneous fit to the SR and TopCR

→ $\sigma_{fid} = 12.2 \pm 1.0(stat)^{+1.9}_{-1.8}(syst)$ fb (5.6σ)

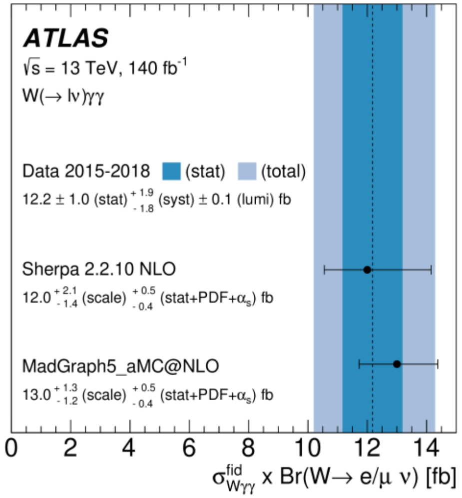

Conclusion

- Precise measurements of the EW VBS can be used as a probe to study the origin of EWSB, especially its longitudinal scattering amplitudes
- ATLAS and CMS experiments have conducted many measurements on EW VBS
  - Cross section measurements (~ fb) and limits on the dimension-8 coefficients in EFT
  - Same-sign WW production (extraction of polarization)
  - Various other channels ($WZ, Z\gamma, W\gamma, \ldots$) and differential measurements
  - Several triboson processes are also becoming available
  - The effort of combining different channels is starting
- We expect more measurements with improved analysis techniques to come

Backup slides

Combined EFT interpretation of $W^\pm Zjj$ and $W^\pm W^\pm jj$

- A single analysis may have good sensitivities for certain EFT coefficients, while other channels may have sensitivities for other coefficients
- We need to combine the results to get the best sensitivities for as wide operators as possible
- In this study, use two datasets of fully leptonic analyses
  - $W^\pm W^\pm + jj \rightarrow l^\pm l^\pm \nu\nu + jj$ (Phys. Rev. Lett. 123 (2019) 161801, 36 pb^{-1})
  - $W^\pm Z + jj \rightarrow l^\pm \nu l^+ l^- + jj$ (Phys. Lett. B793 (2019) 469, 36 pb^{-1})

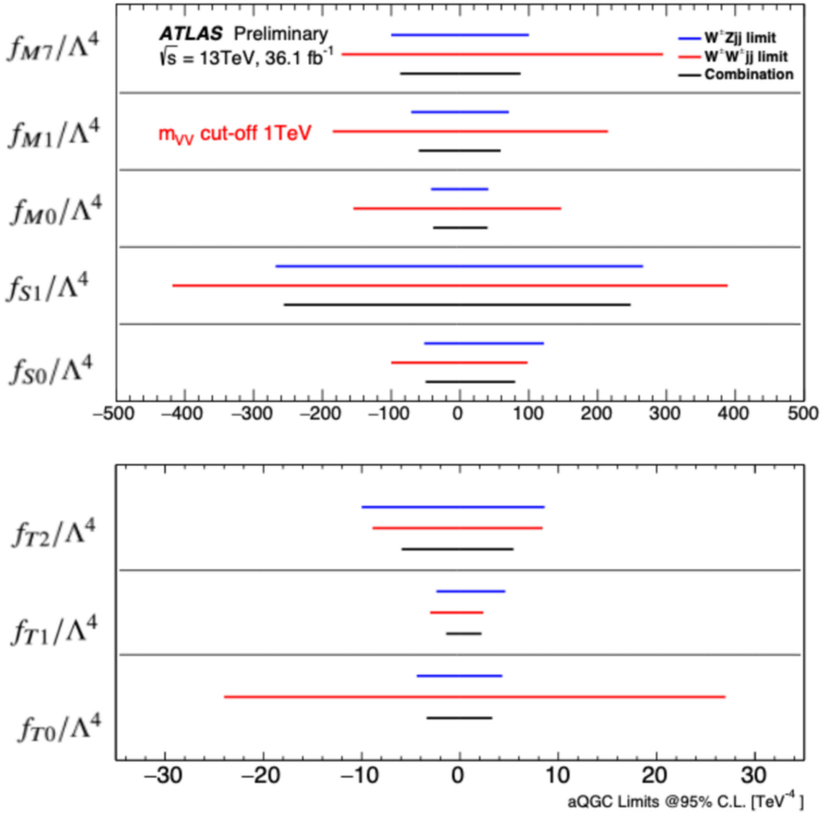

Likelihood for a single measurement:

$$L_b^{WW}\left(N_b\middle|\boldsymbol{c},\boldsymbol{\theta}^{WW}\right) = \text{Poisson}\left(N_b\middle|\mu(\boldsymbol{c})S_b\left(\boldsymbol{\theta}^{WW}\right) + B_b\left(\boldsymbol{\theta}^{WW}\right)\right)$$

For measurements with multiple bins:

$$x_b^{\text{pred}}\left(\boldsymbol{c},\boldsymbol{\theta}^{W^\pm Z}_{\text{theo syst}}\right) = x_b^{\text{SM}}(1+\Delta_b(\boldsymbol{c}))\times\prod^{n^{W^\pm Z}_{\text{theo syst}}}\left(1+\theta_j u_{b,j}\right)$$

$$x_b^{\text{meas}}\left(\boldsymbol{\theta}^{W^\pm Z}_{\text{exp syst}}\right) = x_b\times\prod^{n^{W^\pm Z}_{\text{exp syst}}}\left(1+\theta_j v_{b,j}\right)$$

$$|A_{\text{SM}}+\sum_i c_iA_i|^2 = |A_{\text{SM}}|^2 + \sum_i c_i 2Re(A^*_{\text{SM}}A_i) + \sum_i c_i{}^2|A_i|^2 + \sum_{ij,i\neq j} c_ic_j 2Re(A_iA_j^*)$$

Generate samples for each term with MG5

ATLAS-PHYS-PUB-2023-002

Correlation of parameters of the combined fit

- One can study the correlation of the pair of parameters by having two free parameters
- Uncertainty counters of the combination is reduced from each analysis

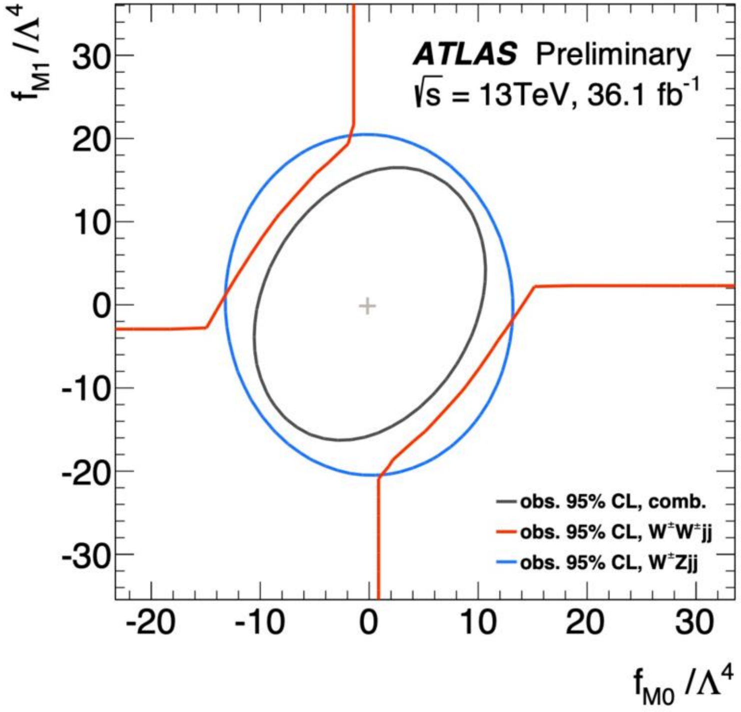

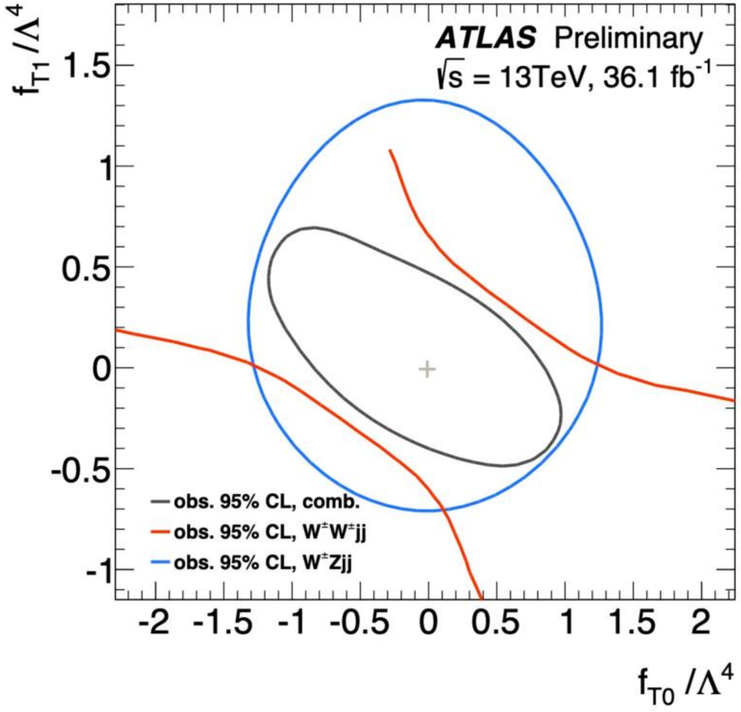

Variables used for the DNN in semileptonic analysis

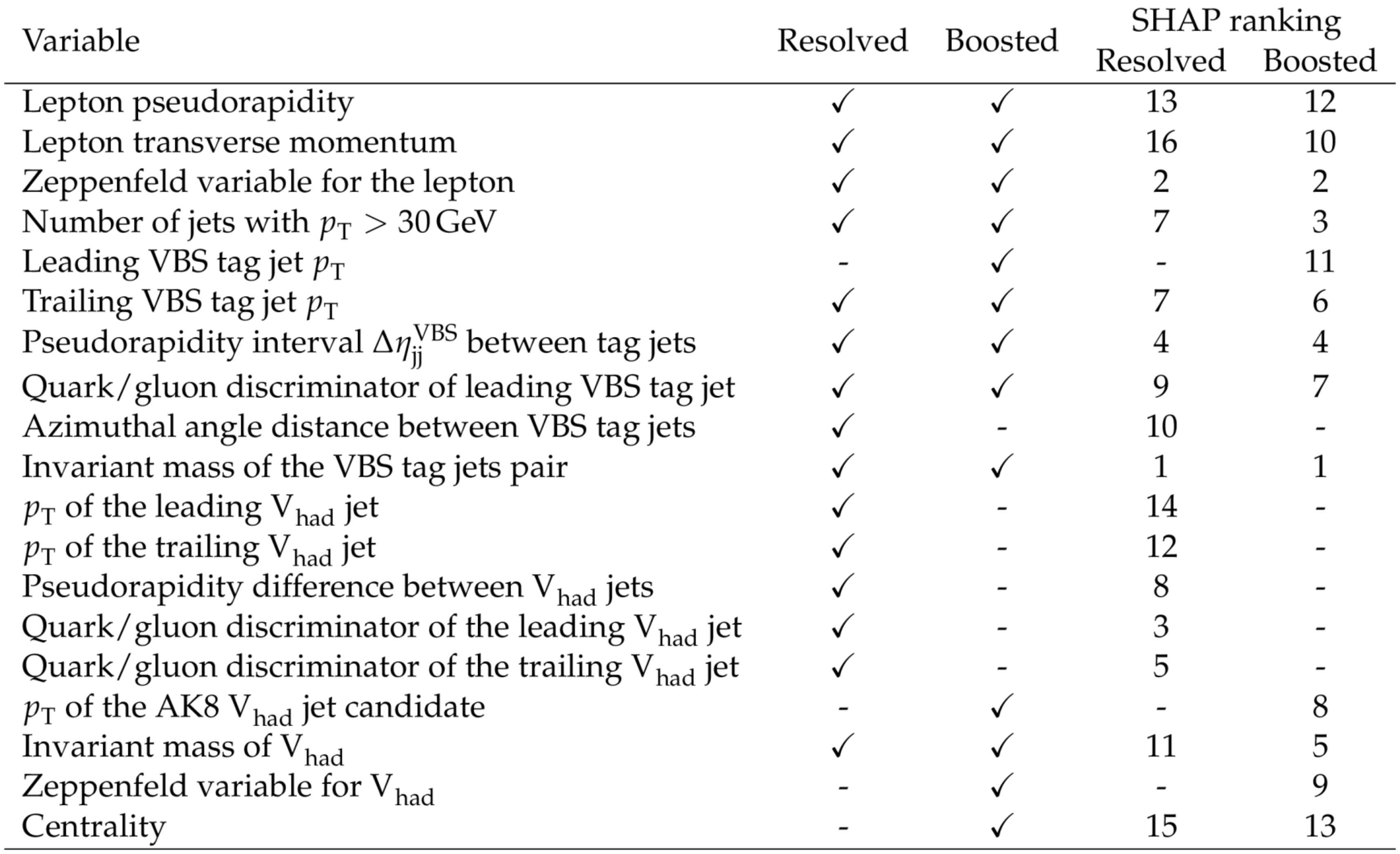

Variable	Resolved	Boosted	SHAP ranking	
			Resolved	Boosted
Lepton pseudorapidity	✓	✓	13	12
Lepton transverse momentum	✓	✓	16	10
Zeppenfeld variable for the lepton	✓	✓	2	2
Number of jets with $p_\mathrm{T} > 30\,\mathrm{GeV}$	✓	✓	7	3
Leading VBS tag jet p_T	-	✓	-	11
Trailing VBS tag jet p_T	✓	✓	7	6
Pseudorapidity interval $\Delta\eta_{\mathrm{jj}}^{\mathrm{VBS}}$ between tag jets	✓	✓	4	4
Quark/gluon discriminator of leading VBS tag jet	✓	✓	9	7
Azimuthal angle distance between VBS tag jets	✓	-	10	-
Invariant mass of the VBS tag jets pair	✓	✓	1	1
p_T of the leading $\mathrm{V}_{\mathrm{had}}$ jet	✓	-	14	-
p_T of the trailing $\mathrm{V}_{\mathrm{had}}$ jet	✓	-	12	-
Pseudorapidity difference between $\mathrm{V}_{\mathrm{had}}$ jets	✓	-	8	-
Quark/gluon discriminator of the leading $\mathrm{V}_{\mathrm{had}}$ jet	✓	-	3	-
Quark/gluon discriminator of the trailing $\mathrm{V}_{\mathrm{had}}$ jet	✓	-	5	-
p_T of the AK8 $\mathrm{V}_{\mathrm{had}}$ jet candidate	-	✓	-	8
Invariant mass of $\mathrm{V}_{\mathrm{had}}$	✓	✓	11	5
Zeppenfeld variable for $\mathrm{V}_{\mathrm{had}}$	-	✓	-	9
Centrality	-	✓	15	13

W mass measurement (reanalysis of 2011 data)

- ATLAS reanalyzed the 2011 data at $\sqrt{s}$ =7 TeV using the improved fitting technique based on profile likelihood test statistics
    - Template fit to p_T^{ll} and m_T distributions
    - m_W lower by10 MeV and total uncertainty lower by 3 MeV

$$\boxed{m_W = 80360 \pm 5(\text{stat}) \pm 15(\text{syst}) \text{ MeV}}$$

ATLAS-CONF-STDM-2023-004

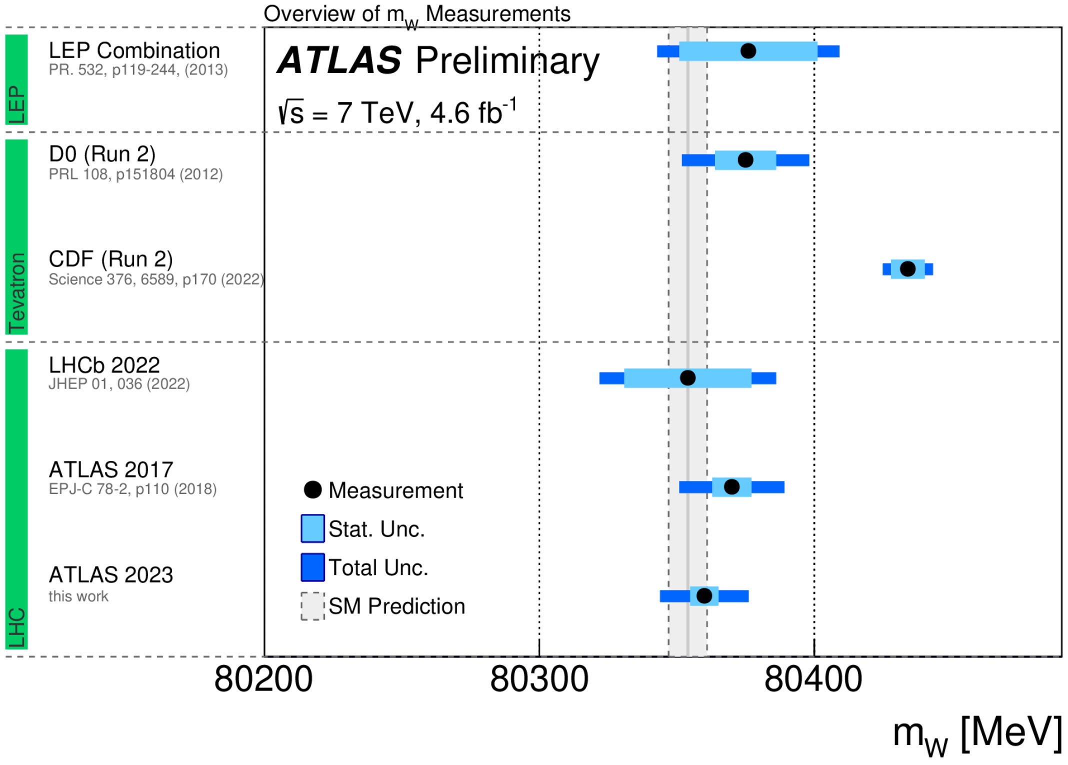

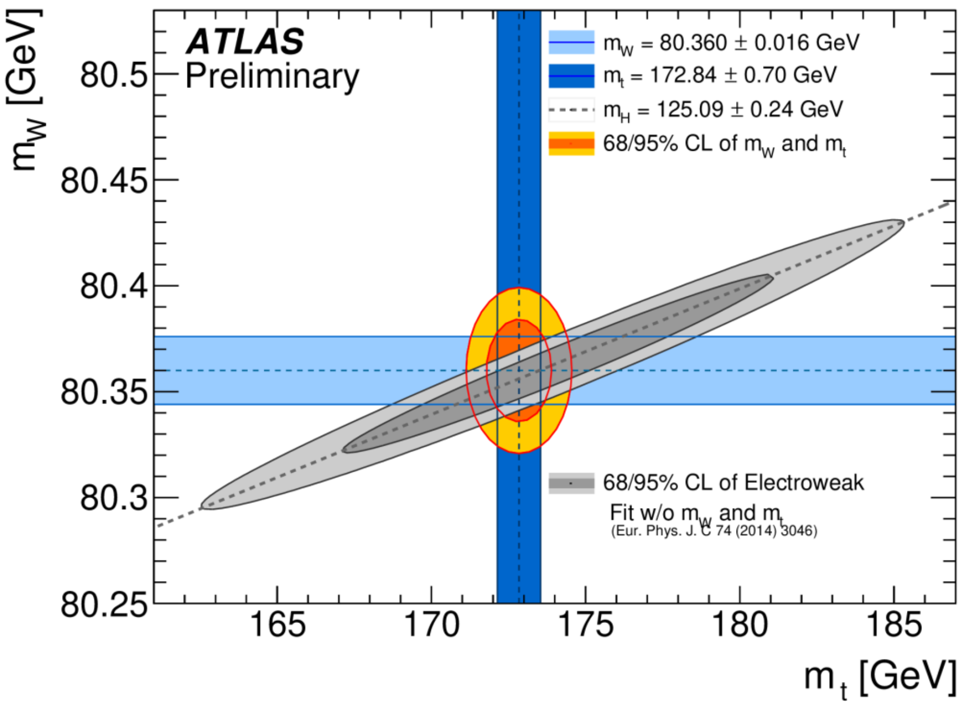

Polarization states in $W^{\pm}Z$ production (1)

- Joint polarization states of $W^{\pm}$ and Z are obtained
- DNN with input variables:
  - $p_{\mathrm{T}}^{l^W}, p_{\mathrm{T}}^{l_1^Z}, p_{\mathrm{T}}^{l_2^Z}, E_{\mathrm{T}}^{\mathrm{miss}}, |y_Z - y_{l^W}|, \Delta\phi(l^W, \nu), \Delta\phi(l_1^Z, l_2^Z), p_{\mathrm{T}}^{\mathrm{WZ}}$
- 4 categories based on $|\cos\theta_{lW}^{*}|, |\cos\theta_{lZ}^{*}|$

Joint helicity fractions

$$f_{00} = 0.067 \pm 0.010$$
$$f_{0T} = 0.110 \pm 0.029$$
$$f_{T0} = 0.179 \pm 0.023$$
$$f_{TT} = 0.644 \pm 0.032$$

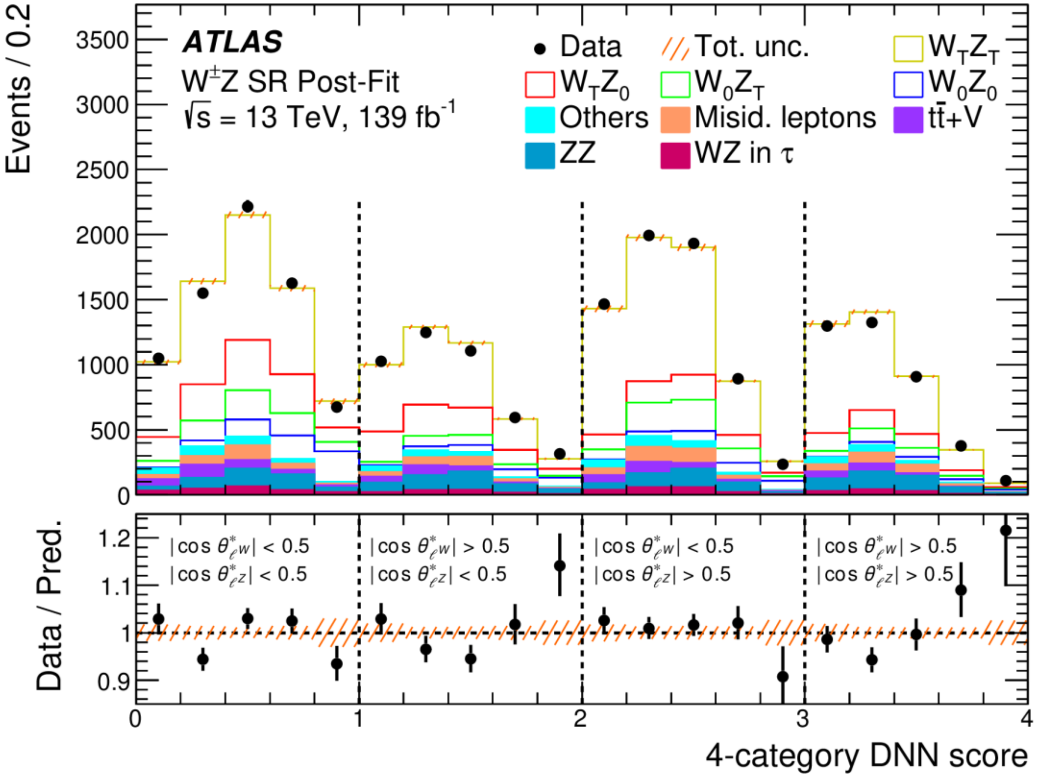

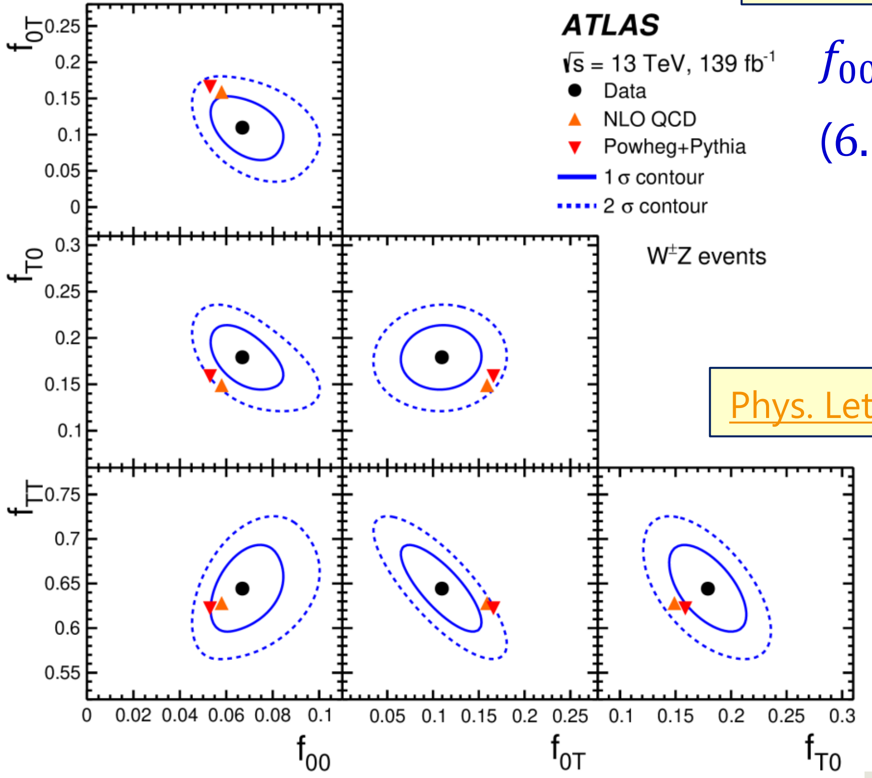

f_{00} is observed at 7.1σ (6.2σ expected)

Phys. Lett. B 843 (2023) 137895

Polarization states in $W^{\pm}Z$ production (2)

- Inclusive cross section: $\sigma_{W^{\pm}Z\rightarrow l^{\pm}\nu l^{+}l^{-}} = 64.6 \pm 0.5(\text{stat}) \pm 1.8(\text{syst}) \pm 1.1(\text{lumi})$ fb
- Post-fit distributions $q_W \cdot \cos\theta^*_{lW}$ and $\cos\theta^*_{lZ}$
- Differential cross sections: $q_W \cdot \cos\theta^*_{lW}$, $\cos\theta^*_{lZ}$, $|\cos\theta_V|$ and DNN score